Error analysis and modelling of non-linear stress–strain behaviour in measuring dynamic mechanical properties of polymers with the Rheovibron

Alan R. Wedgewood and James C. Seferis*
Department of Chemical Engineering, University of Washington, Seattle, Washington 98195, USA
(*Received* 27 *June* 1980; *revised* 17 *October* 1980)

The Rheovibron is widely used for measuring the dynamic mechanical properties of polymers. Poor reproducibility and data variation which have been considered inherent to the Rheovibron operation necessitate both instrument modifications and modelling of the instrument operation for quantitative interpretation of the experimental data. The instrument modifications that have been made in this study include electronic modifications, a new clamp design that eliminates sample mounting and slippage problems, and the design of an environmental chamber, which, along with a nitrogen purge, eliminates moisture condensation on the sample at low temperatures. A previously-developed mathematical model for the instrument has also been extended to account for the effect of the static stress and the stress rate imposed on the sample during measurement. Based on a simple constitutive relation for non-linear stress–strain behaviour of polymers, this model has been applied to a number of polymeric materials including polyethylene, polyimide, poly(ethylene terephthalate), and polypropylene, among others. The instrument modifications and modelling of the influence of static stress and the stress rate imposed on the sample during dynamic mechanical testing allows for reproducible (within 5%) and accurate use of the Rheovibron.

INTRODUCTION

The Rheovibron viscoelastometer has been extensively used for measuring the extensional dynamic mechanical properties of polymeric materials. Studies have extended the instrument's capabilities to shear and bending test modes[1–4], and to measurements under different environments[5,6]. The instrument's range and reproducibility have also been improved through new electronics[7,8] and automatic operation[8]. A comprehensive list maintained by the US distributor (Imass, Accord, Mass.) lists over 400 papers that have been published making use of the Rheovibron. In spite of its wide use, attention has rarely been directed to the changes and artifacts that the instrument can impose on the polymeric sample during measurements.

Dynamic mechanical data obtained with the Rheovibron can show discrepancies of the order of 30% to 50%, depending on how familiar the operator is with the instrument's operating procedure. These large data variations have prompted several investigations[1,2,7,8] into the sources of the instrument's poor reproducibility, which may be attributed to: (a) the compliance of the instrument; (b) yielding and slippage of the sample in the clamps; (c) sample misalignment; (d) the instrument's inertia; (e) the use of variable sample dimensions; and (f) structural changes imposed on the sample during testing. A comprehensive study by Massa, who proposed a mechanical model analogue of the instrument[1], and a number of apparatus modifications[2], both to explain rationally and eliminate some of this data variation. In spite of Massa's efforts, poor data reproducibility may still be observed, primarily due to changes imposed on the sample during testing. These changes can be disturbing in studies which attempt to correlate the internal architecture of a polymeric sample with its dynamic mechanical properties[9–12]. In such studies, the internal structure of the sample is identified and described before testing. Consequently, a quantitative interpretation of the polymer's dynamic mechanical properties, in terms of its internal structure, assumes that the sample's structure was not changed during the measurement. However, the basic principle of Rheovibron operation[13,14], requires that a static displacement, which is greater than the oscillating displacement, be imposed on the sample during testing. These displacements will result in static and dynamic deformations which can be expressed as either stress or strain functions whose magnitudes will depend on the sample dimensions and the properties of the polymer used. Since the magnitude of the static strain (or stress) and/or the oscillating strain (or stress) amplitude can affect the internal structure of a polymeric sample[14–16] and thus the properties measured, a procedure is required to obtain dynamic mechanical data at a state of deformation, described either in terms of stress or strain, in which the internal structure of the sample is not changed. In previous studies on polypropylene[10–12], a number of instrument modifications and a set of empirical rules were developed that allowed for the extrapolation of dynamic mechanical data to a deformation-free state. Here, these empirical rules have been quantitatively expressed, so that the influence of the applied static and oscillating deformations on the measured dynamic mechanical properties can be examined for any polymer.

* To whom correspondence should be addressed

0032-3861/81/070966-26$02.00

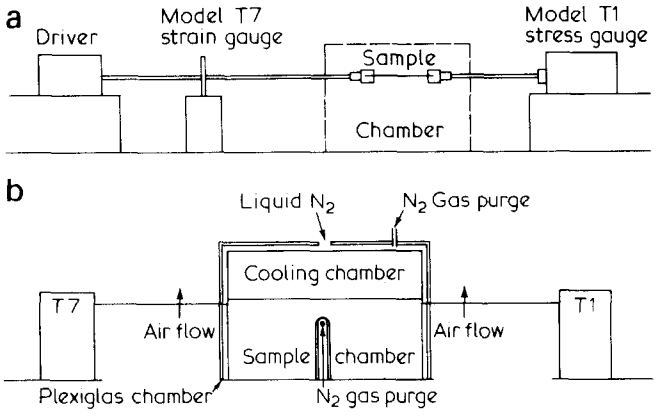

Figure 1 Schematic diagrams of the Rheovibron: (a) T1 and T7 are unbounded type wire strain transducers that monitor the stress and strain, respectively. (b) Sample chamber showing the plexiglass enclosure and air flow to the rods that connect the sample to the gauges

EXPERIMENTAL

Dynamic mechanical experiments were performed with a Rheovibron dynamic viscoelastometer, model DDV-IIB. This instrument, originally developed by Takayanagi[13], and manufactured by the Toyo Measuring Instrument Co. Ltd (Tokyo), is marketed in the US by Imass (Accord, Mass.). Several newer models have appeared on the market since the introduction of DDV-IIB. These include model DDV-IIC (a solid-state version of the model DDV-IIB) and model DDV-III (a modified instrument to handle larger samples). The principle of operation and the basic instrument design is the same for all models of the Rheovibron, as well as most 'homemade' instruments that have been used for measuring the dynamic mechanical properties of polymers. Although not without problems, the Rheovibron, due to its wide use and ease of operation, has made an important contribution to the polymer field, by allowing for the direct comparison of data from different laboratories. This was not always possible before the introduction of the Rheovibron, when each investigator had to make his own instrument for dynamic mechanical measurements. Frequency differences and specific errors arising from each particular instrument design made direct comparison of dynamic mechanical data difficult. By adapting the Rheovibron design, these difficulties can be resolved.

Principle and method of operation

A systematic analysis of the instrument's basic principle and operation, is provided as a starting point for considering in depth the various factors that contribute to the errors observed in the dynamic mechanical data measured with the Rheovibron. A schematic of the Rheovibron instrument emphasizing its principle components is provided in *Figure 1a*. The instrument operation is based on the general principle of extensional, forced oscillation mechanical measurements, and can be summarized as follows: A polymeric sample is mounted and properly aligned within the sample holders. A small sinusoidal displacement, at a selected frequency, is then applied to one end of the sample by the driver. This displacement is monitored by the T7 strain transducer and can be generally described in complex exponential form as:

$$X = X_0 e^{i\omega t} \tag{1}$$

where X_0 and ω are the amplitude and angular frequency, respectively.

To ensure that the desired displacement amplitude is obtained, the power output of the driver is adjusted with an amplitude adjust dial, while the T7 transducer output is matched to an internal calibrated reference signal[14]. To prevent the sample from buckling, a static displacement greater than the oscillating displacement amplitude is simultaneously imposed on the sample.

The Rheovibron is capable of operating at several oscillating displacement amplitudes, X_0 (e.g. 0.0016, 0.005 and 0.016 cm), and four discrete frequencies (e.g. 3.5, 11, 35 and 110 Hz)[14]. In addition, operation over the continuous frequency range between 0.01 and 1 Hz can be achieved using the low frequency attachment available from the manufacturer. Unfortunately, it has been observed[2] that the 35 Hz frequency is the instrument resonance frequency for lateral vibrations, and even though resonance clips are available, this condition has limited use primarily to frequencies of 3.5, 11, and 110 Hz. For each frequency measurements can be made as a function of temperature and the temperature is controlled by the heaters located in the sample chamber or by introducing liquid nitrogen into the cooling chamber, that is in direct contact with the sample chamber (see *Figure 1b*).

The sinusoidal force response is monitored, at the other end of the sample, by the T1 stress transducer (*Figure 1*). For a viscoelastic material, this force response will lead the applied displacement by a characteristic phase angle δ, which is bounded in the interval $0 \leqslant \delta \leqslant \pi/2$ (since $\delta = 0$ for a perfectly elastic solid and $\delta = \pi/2$ for a perfectly viscous fluid). Consequently, the phase angle δ provides a unique measure of the polymer's viscoelastic behaviour at the temperature and frequency of experimentation. However, as discussed by Massa[1], the phase angle measured by the Rheovibron is influenced by the instrument components and in general is not equal to the unique material phase angle δ. Massa denoted the measured phase angle by α, to distinguish it from the material phase angle δ. Using this notation, the force response measured by the T1 transducer can be expressed in complex exponential form as:

$$F = F_0 e^{i(\omega t + \alpha)} \tag{2}$$

where F_0 is the amplitude of the oscillating force response.

The signals from the T1 and T7 transducers are converted by the instrument electronics to give a direct readout of the tangent of the measured phase angle (tan α). The instrument also provides a potentiometer reading D, which is inversely proportional to the force amplitude F_0[14]. D is generally referred to as the dynamic force and has a relative range of 0–1000 units. Using the measured force amplitude F_0, the applied displacement amplitude X_0, and the sample dimensions, the magnitude of the complex modulus $|E^*|$ and/or complex compliance $|S^*|$ can be calculated from the following relationship:

$$|E^*| = \frac{1}{|S^*|} = \frac{F_0}{X_0}\frac{L}{A} \tag{3}$$

where L is the sample length and A is its cross-sectional area. It should be noted that in equation (3) L refers to the length of the sample between the clamps and includes the small static displacement imposed on the sample during a measurement. The amplitudes of the oscillating force and

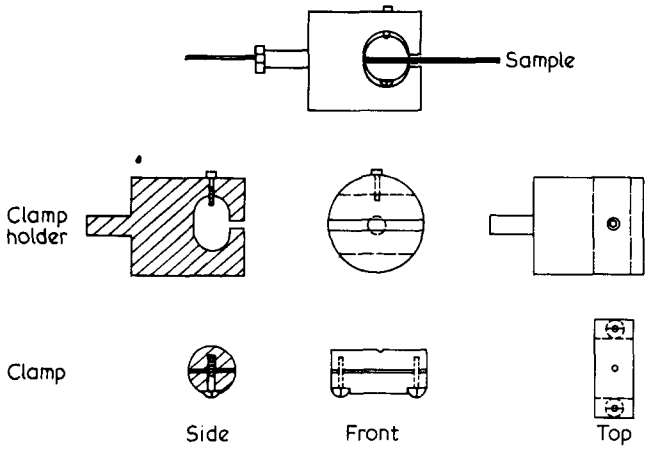

Figure 2 Projections of the sample clamp for the Rheovibron: clamp and holder assembly, clamp holder, and clamp

displacement can be expressed in terms of instrument calibration constants[14] as:

$$X_0 = 5.0 \times 10^{-3}(AF)N \text{ (units of cm)} \quad (4)$$

$$F_0 = 1.0 \times 10^{7} N/D \text{ (units of dynes)} \quad (5)$$

where AF and N are instrument amplification factors. Substitution of (4) and (5) into equation (3) gives the magnitude of the complex modulus and/or complex compliance in terms of instrument and sample geometry parameters:

$$|E^*| = \frac{1}{|S^*|} = \frac{2 \times 10^9}{D(AF)} \frac{L}{A} \text{ (units of dyne cm}^{-2}\text{)} \quad (6)$$

This equation assumes that the material in the clamps, the instrument compliance and inertia, all make negligible contributions to the measured modulus or compliance for the sample. Equation (6) also implies that if the measured complex modulus or compliance are independent of the dimensions of the sample tested, a plot of $D(AF)$ *versus* L/A should be linear. The slope of this line should be inversely proportional to the complex compliance and its intercept should be at $D(AF)=0$. Although in practice a linear relation between $D(AF)$ and L/A is observed, the intercept value can be significantly different from zero. This intercept value has been termed the 'error constant', and is designated D_0. The error constant is a consequence of the indirect attachment of the sample to the stress and strain transducers[1,14], and depends on the specific polymeric material being tested, the experimental frequency, and the temperature of experimentation. Equation (6) may be modified to incorporate the error constant, D_0, yielding the complex modulus or compliance as:

$$|E^*| = \frac{1}{|S^*|} = \frac{2 \times 10^9}{D(AF) - D_0} \frac{L}{A} \text{ (units of dyne cm}^{-2}\text{)} \quad (7)$$

The determination of the error constant, as described in the instruction manual[14], involves linear extrapolation of the values of $D(AF)$ as a function of sample length, L, to the value of $L=0$. As discussed earlier, this procedure will only be valid for samples with the same cross-sectional area. If samples of variable cross-sectional area are used, equation (7) suggests that the values of $D(AF)$ should be plotted as a function of L/A and extrapolated to $L/A=0$. Either of these procedures should result in the determination of a unique error constant, D_0, independent of sample geometry. However, experimental results in this study have shown that the error constant is dependent on the sample geometry within the clamps. Consequently, a modification of these extrapolation procedures is required, incorporating the dependence of the error constant on the sample dimensions within the clamps. A modified extrapolation procedure will be provided below.

Experimental factors considered so far imply that experiments on samples from the same polymeric material with identical geometries should provide identical results. However, this may not always be the case in practice, where dynamic mechanical data obtained with the Rheovibron for identical samples can still have discrepancies of the order of 30%. To eliminate these descrepancies, several modifications and an operating procedure were developed in the course of our experimental work. These modifications, which are summarized below, resulted in reproducible data (within 5%) when identical samples were tested with the Rheovibron.

Instrument modification

The modifications made were: a new clamp design, elimating sample slippage and ensuring proper alignment; the design of an environmental chamber which, along with a nitrogen purge, eliminated moisture condensation and freeze-up on the sample at low temperatures; electronic modifications that improved the sample monitoring capabilities during operation; and an experimental method for measuring the static force or displacement applied to the sample during testing.

New clamp design. Poor reproducibility in Rheovibron experiments to a large extent can be attributed to sample slippage in the clamps and poor sample alignment. The clamping assembly shown in *Figure 2* was developed to minimize these effects. Each clamp consists of two half cylinders that are tightened together about the sample with a pair of screws. After the sample has been mounted, and properly aligned between the clamps, any excess material protruding from the back of the clamps is trimmed away. The clamps and sample are then mounted into the clamp holders, which are directly connected to the transducer rods. A snug fit, along with a set screw, prevents the clamps from moving within the holders during the course of an experiment. This clamp design differs from the original clamping system provided with the Rheovibron, in that the sample can now be mounted and aligned away from the instrument. Consequently, unnecessary disturbance to the transducers are eliminated. In addition, the trimming procedure provides for a constant sample length within the clamps from one sample to the next. Furthermore, if care is taken, so that the width for each of the samples used is approximately equal to the clamp width (~ 0.5 cm), the clamping area can be maintained constant from one sample to the next. Both the clamps and clamp holders can be made from aluminium or stainless steel. However, it has been proven that it is preferable to use aluminium for the clamp holders in order to reduce weight and stainless steel for the clamps to minimize their distortion which results from multiple sample mountings. Use of this clamp design[10-12,17-21], has resulted in enhanced reproducibility of the data

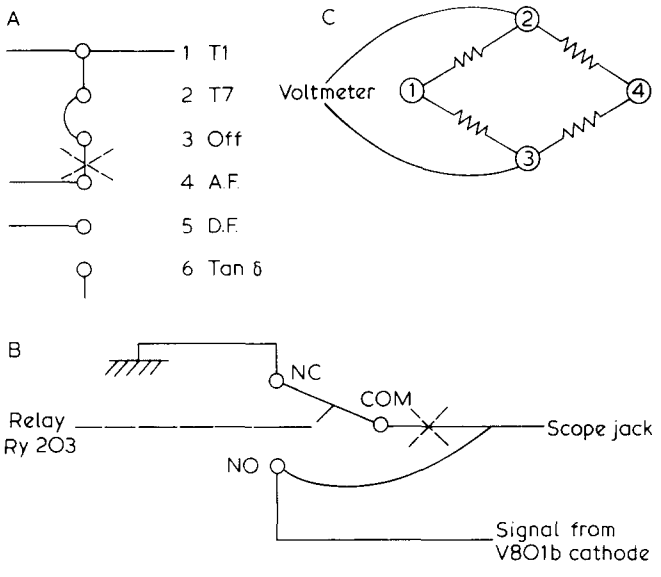

Figure 3 Circuit diagrams of electronic modifications: A, Main Selector Switch (SW 301a); B, Oscilloscope connection; C, T1 stress gauge. In diagrams, broken crosses denote connections to be broken, and curved solid lines denote new connections

obtained with the Rheovibron, due to the improved sample mounting and alignment discussed above and the elimination of significant sample slippage.

Environmental chamber. Low temperature operation of the Rheovibron is usually accomplished by introducing liquid nitrogen into a rectangular open-faced cooling chamber, which is in direct contact with the sample chamber (*Figure 1b*). Heaters located in the bottom of the sample chamber allow for high temperature operation and the control of the heating rate. This chamber assembly is widely used with the Rheovibron DDV-II, and is commercially available from Imass. During low temperature operation, dry nitrogen is introduced into the sample chamber to prevent moisture from freezing on the sample. However, it has been observed that upon slow cooling, ambient moisture condensing on the sample and cooling chambers could also be deposited on the sample itself through the contact areas of the two chambers. Upon further cooling a frost layer would form on the sample, drastically affecting its measured dynamic mechanical properties. This moisture condensation and freeze-up problem has been eliminated using a Plexiglass chamber which tightly encased both the cooling and sample chambers, as shown in *Figure 1b*. Both the Plexiglass chamber and the sample chamber are continuously purged with dry nitrogen gas during low temperature operation preventing condensation and frost from forming on the outside of the sample and cooling chambers. *Figure 1b* also shows a small sealable port on top of the Plexiglass chamber which allows the introduction of liquid nitrogen into the cooling chamber. Also, by keeping the dry nitrogen purge active during high temperature operation, possible oxidation of the sample can also be avoided.

In addition to constructing the environmental chamber, it was also found advantageous to blow room temperature air gently across the transducer rods to prevent heat conduction to or from the transducers. The resulting air convection has been found very effective in eliminating variations in the transducer's temperature, and thus measurement errors caused by variations in the transducer's response with temperature. Finally, during continuous operation from low to high temperatures at a specified heating rate of 1°C min^{-1}, temperature gradients between the top and bottom of the sample chamber as large as 15°C were observed[18]. These gradients were attributed to the fact that the heaters are located only at the bottom of the sample chamber. To ensure that the sample is exposed to a uniform temperature profile during testing, it was found necessary to add a strip heater to the cooling chamber. Temperature gradients were thus eliminated, and the data reproducibility was greatly improved by maintaining a uniform temperature around the sample.

Electronics. The electrical outputs from the stress and strain gauges are directed through a multiple switch, called the main selector switch, to a multipurpose voltmeter (tanδ-meter) for calibration, balancing, and measurements[14]. The positions that the main selector switch can assume are schematically illustrated in *Figure 3a*. During the course of an experimental run, balancing and reading of the voltmeter values are carried out only when measurements are being made. Between measurements, the main selector switch is kept in the off position. However, operation in the OFF position on the main selector switch did not stop the driver oscillations for the original design. This continuous oscillation was found to cause variation in the measured properties due to excessive working of the sample. Although this effect can by eliminated by loosening the sample between measurements, it is easier, from an operational point of view, to have the driver shut off when the main selector switch is placed in the OFF position. A simple rewiring of the main selector switch can add this capability to the instrument. As shown in *Figure 3a*, rewiring involves the elimination of the connection between points 3 and 4, followed by the connection of points 2 and 3.

The circuit arrangement of the Rheovibron, as an aid to the balancing operation, can also provide for monitoring of the outputs from the stress and strain gauges through an oscilloscope. In the original instrument design, this monitoring capability is only available at the dynamic force (*DF*) position of the main selector switch. To expand this monitoring capability to all positions of the main selector switch, the simple rewiring of the circuit shown in *Figure 3b* was performed. This modification involves connecting the scope jack to point NO rather than COM, as in the original design. With this minor change, the Rheovibron operator can monitor instrument output in each operating mode, using an oscilloscope. The resulting Lissajous figures observed with the oscilloscope can assist in detecting sample shrinkage, sample misalignment, and lateral vibrations. To assist future users with this new monitoring capability, further discussion of the Lissajous figures is provided in the Appendix.

Static force measurement. Operation of the Rheovibron requires that a static displacement be imposed on the sample during testing. Consequently, for reproducible operation, the ability to impose and monitor the same static displacement (or force) histories on samples that are tested at different times and by different operators is essential. A simple procedure was developed to monitor both the static displacement and the static force applied to

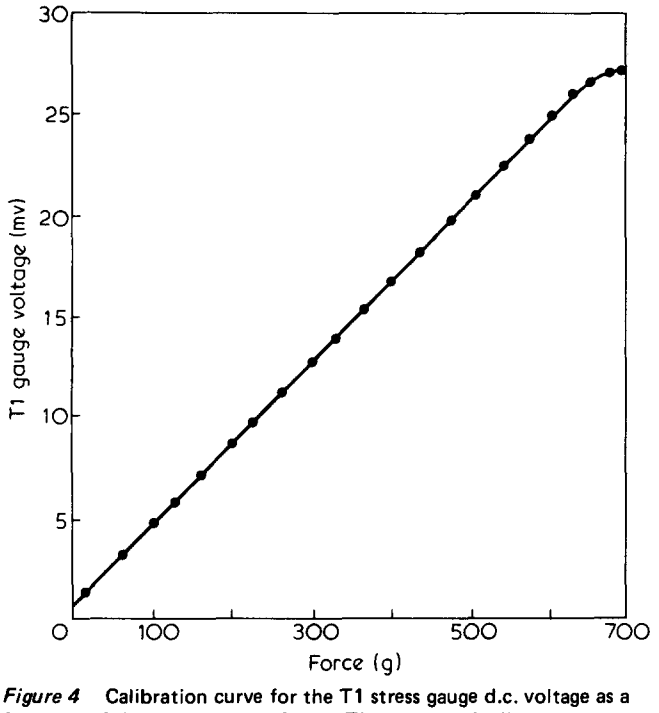

Figure 4 Calibration curve for the T1 stress gauge d.c. voltage as a function of the applied static force. The slope in the linear range is 0.04 mV g^{-1}

the sample during a measurement. This procedure involves the measurement of the d.c. voltage across connections 2 and 3 of the T1 stress gauge (*Figure 3c*), while the sample is in its extended position and the driver is in the OFF position. By applying various known loads to the T1 stress gauge, and measuring the corresponding voltage output, the calibration curve provided in *Figure 4* was obtained. The voltage response of the T1 stress gauge varies linearly with the applied force up to a force level of 620 g, which corresponds to the gauge limit specified by the manufacturer[14]. In generating the calibration curve, it was observed that the T1 stress gauge had a 'floating zero' and thus the output at zero load was not constant. Consequently, the zero load value, which ranged between 0.75 and 0.85 mV, was redetermined periodically, especially when small forces were being monitored. The above procedure, along with the calibration curve provided in *Figure 4*, can be used to measure directly the static force imposed on the sample during testing.

This procedure can also be extended to provide an experimental determination of the corresponding static displacement on the sample. What must be determined is the value of the unstrained sample length which can be subtracted from the sample length in tension to yield the corresponding displacement. The Rheovibron's built-in length dial[14] provides a reading of the sample length with tension at the time of measurement. The unstrained sample length can also be determined with the instrument's length dial as follows. Starting with the sample loosely held (no tension) between the clamps, incremental extensional displacements are applied to the sample. The unstrained sample length can then be read, with the instrument's length dial, as the point at which the T1 stress gauge output voltage begins to change from its zero load value. Although this technique for measuring the unstrained sample length has been independently verified by measuring the unstrained sample length with vernier calipers, it suffers from the inconvenience that the sample must be loosened before each measurement. In addition, the measured displacement is distributed between the instrument components and the sample both within and between the clamps. The procedure for the determination of the static displacement is difficult to apply during an experimental run in which the continuous heating of the sample results in large changes in the sample dimensions. However, at low temperatures where most polymers are dimensionally stable, this procedure can be applied to the determination of the unstrained sample length. Although the measurement of either the applied static force or displacement enables the operator to monitor and control the experimental conditions, it is clear that it is more convenient to monitor the applied static force in order to ensure reproducible operation of the Rheovibron.

QUANTITATIVE DESCRIPTION

The analysis and instrument modifications considered above addressed the problem of obtaining reproducible dynamic mechanical data for samples from the same polymer having identical geometries and measured under the same experimental conditions (i.e. temperature, heating rate, frequency, static stress, etc.). What needs to be considered, in conjunction with the reproducibility problem, is the fact that the dynamic mechanical properties measured with the Rheovibron may not be the true material properties. Conditions imposed by the instrument on the polymeric sample during testing may alter reversibly or irreversibly the sample itself. In addition, the influence of the instrument's components may introduce systematic errors in the measured dynamic mechanical properties. As noted earlier, the deformation of the sample in the clamps as well as the instrument compliance and inertia must be accounted for when calculating the true material dynamic mechanical properties. In order to take into account how these conditions affect the measured properties, a quantitative description of the instrument and the influence of its operation on the measured dynamic mechanical properties is required. The sections that follow provide a mathematical model that can quantitatively describe these effects.

Modelling instrument response and operation

The influence of the instrument's components, shown schematically in *Figure 5a*, on the measured dynamic mechanical properties were accounted for through a mechanical model analogue. In *Figure 5b*, a translation of this physical system into a series arrangement of mechanical spring elements, each of which has an appropriate spring constant associated with it, is provided. In *Figure 5c*, the mechanical model analogue proposed by Massa[1] to describe the dynamic operation of the Rheovibron is shown. He accounted for the instrument's response in the calculation of dynamic mechanical properties measured with the Rheovibron. Massa's model represented the instrument's compliance by a single spring constant S_m^0, and the system's inertia by a mass M. The sample's response was modelled by a single dynamic spring constant K^*, which represented the dynamic response for the sample within and between the clamps. By modelling K^* as a simple linear dynamic spring, Massa showed that the equation of motion for this mechanical system was:

$$M\ddot{X}_1 = K^*(X - X_1) - S_m^0 X_1 \qquad (8)$$

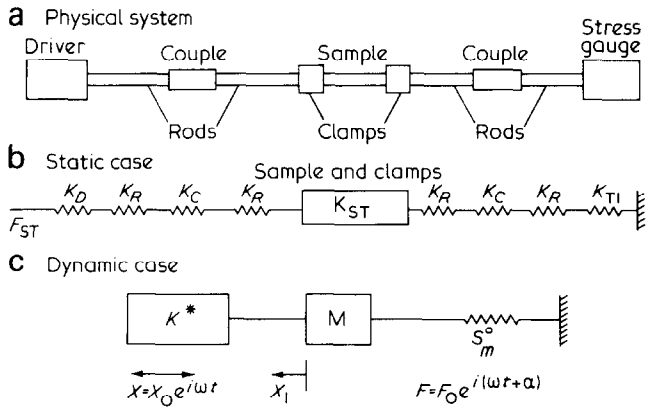

Figure 5 Schematic diagram of the Rheovibron components taken into account in mathematical modelling; (a), physical description of the instrument's components; (b), representation of the instrument components by a series of mechanical springs; (c), the mechanical model analogue proposed by Massa[1] to describe the instrument's dynamic operation

Assuming the steady state solution, $F=F_0e^{i(\omega t+\alpha)}$ and $X=X_0e^{i\omega t}$, Massa obtained an analytical solution to the equation of motion, and provided the following expressions for an instrument-free material complex modulus (in units of dyne cm^{-2}) and tan δ:

$$|E^*|=\frac{2\times10^9\left(1-\frac{M\omega^2}{S_m^0}\right)}{(AF)\left\{D\left[1+\left(\frac{D_{oc}}{D}\right)^2-2\left(\frac{D_{oc}}{D}\right)\cos\alpha\right]^{1/2}-D_{ov}\right\}}\left(\frac{L}{A}\right) \tag{9a}$$

$$\tan\delta=\left(1-\frac{D_{oc}}{D\cos\alpha}\right)^{-1}\tan\alpha \tag{9b}$$

As discussed earlier this equation states that the measured tangent of the phase lag angle, tan α, differs from the true material descriptor, tan δ. In these expressions D_{oc} and D_{ov} are the constant and variable components of the error constant D_o, respectively. The error constant D_o is provided by the sum of these components, i.e.:

$$D_o=D_{oc}+D_{ov} \tag{10a}$$

which were also provided by Massa in terms of model and instrument parameters as:

$$D_{oc}=\frac{2\times10^9}{S_m^o(AF)} \tag{10b}$$

$$D_{ov}=\frac{2\times10^9\left(1-\frac{M\omega^2}{S_m^o}\right)}{|K_o^*|(AF)} \tag{10c}$$

In equation (10c), the constant $|K_o^*|$ denotes the magnitude of the dynamic spring constant for the sample in the clamps, and was appropriately defined by Massa[1] as:

$$|K_o^*|=\lim_{L\to0}|K^*| \tag{11}$$

As can be seen from equation (10b), the first component of the error constant, D_{oc}, should be constant, since it depends only on the instrument compliance. In contrast, since the second component, D_{ov}, is inversely proportional to the dynamic spring constant for the sample within the clamps, it depends on the polymeric material being tested, the experimental frequency, and the temperature of experimentation.

Massa's results were also expressed in the traditional storage E', and loss E'' moduli, which may be defined from complex arithmetic as:

$$E=|E^*|\cos\delta \tag{12a}$$

$$E''=|E^*|\sin\delta \tag{12b}$$

with

$$E^*=E'+iE'' \tag{12c}$$

$$|E^*|=(E'^2+E''^2)^{1/2} \tag{12d}$$

From the above equations, the storage and loss moduli can be related to the model constants and instrument parameters viz.,

$$E'=\frac{|E^*|\left(1-\frac{D_{oc}}{D\cos\alpha}\right)}{\left[1+\left(\frac{D_{oc}}{D}\right)^2-2\left(\frac{D_{oc}}{D}\right)\cos\alpha\right]^{1/2}}\cos\alpha \tag{9c}$$

$$E''=\frac{|E^*|}{\left[1+\left(\frac{D_{oc}}{D}\right)^2-2\left(\frac{D_{oc}}{D}\right)\cos\alpha\right]^{1/2}}\sin\alpha \tag{9d}$$

Similarly, the above results can also be expressed in terms of the storage and loss compliance, which in complex arithmetic are defined as:

$$|S^*|=S'-iS'' \tag{13a}$$

with

$$S'=|S^*|\cos\delta \tag{13b}$$

$$S''=|S^*|\sin\delta \tag{13c}$$

$$|S^*|=(S'^2+S''^2)^{1/2} \tag{13d}$$

The advantage of using dynamic compliances, rather than moduli, has been amply demonstrated in studies that correlate polymer's internal structure with dynamic mechanical properties[10-12]. From complex arithmetic the dynamic compliances can simply be related to the dynamic moduli by the following relations:

$$S'=\frac{E'}{E'^2+E''^2} \tag{14a}$$

$$S''=\frac{E''}{E'^2+E''^2} \tag{14b}$$

These expressions for compliance can be used in conjunction with equation (9) to take into consideration the

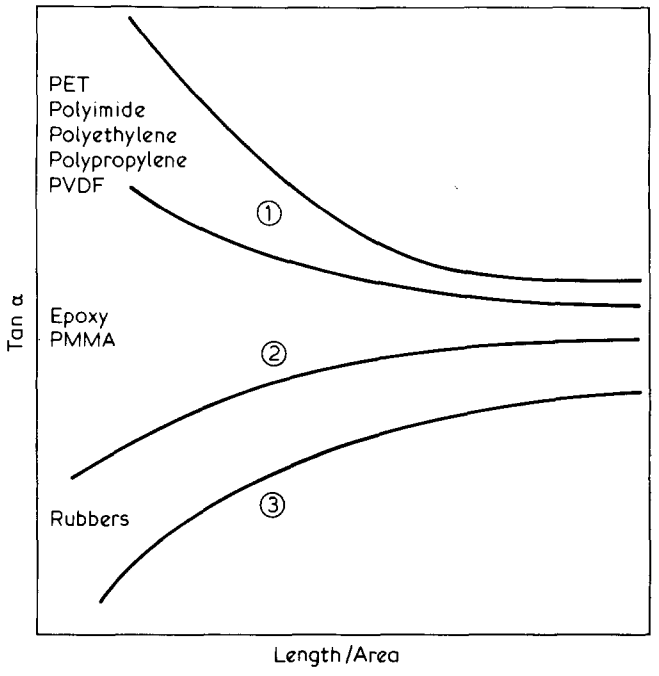

Figure 6 Schematic representation of the dependence of the measured loss tangent (tan α), on the sample geometry (*L/A*). Depending on the temperature and the polymer studied, tan α was found to either increase, decrease, or remain unchanged with *L/A*. Scales for tan α and *L/A* are relative

effects of the instrument components on the measured dynamic compliance.

Massa's results predicted for the first time that the measured complex modulus, $|E^*|$, and tan α would be influenced by the instrument components and the sample geometry (L/A). In particular, the model predicted tan α to increase with increasing L/A, reaching as an asymptotic limit the true material value, tan δ, at large L/A. However, when Massa applied his model to the dynamic mechanical data obtained for poly(methyl methacrylate) (PMMA), he observed that tan α was independent of the sample geometry used. Although this result was inconsistent with the model prediction, Massa[1] was unable to offer an explanation for this discrepancy.

In our experimental work, the Rheovibron has been used to investigate polyethylene[17], polypropylene[10-12,18,21], epoxy[19,20] and a variety of other polymeric materials[21]. For all of these polymers, we have investigated the effect of sample dimensions (L/A) on the measured dynamic mechanical properties, and have observed a number of distinct trends. As shown schematically in *Figure 6*, tan α was observed either to increase, decrease, or remain constant with decreasing L/A, depending on the specific polymer tested. The trends shown for the various polymers in *Figure 6* correspond to room temperature results (20°C), with the exception of the rubber data of Ramos *et al.*[22], which were observed at −55°C. The trends for the specific polymers shown in *Figure 6* are valid only for the temperature given, and may change with temperature. For example, we have observed[21] that poly(vinylidene fluoride) (PVDF) exhibits a decrease in tan α with decreasing L/A, below −24°C, while above this temperature the opposite is true. In contrast, poly(ethylene terephthalate) (PET) exhibits an increase in tan α with decreasing L/A, for temperatures ranging from −120° to 80°C, as shown in *Figure 7*. Above 80°C, the trend with sample geometry for PET is not discernable. It should also be noted that for all the materials examined, tan α was found to approach an asymptotic limit at large L/A, which is consistent with Massa's model prediction. Also as will be shown later, this asymptotic limit for tan α corresponds to the material's linear viscoelastic properties.

The measured complex modulus and compliance were also found to be dependent on sample dimensions. However, no uniform trends with L/A were observed for the different polymers studied.

These observations show that the effects of sample geometry on the dynamic mechanical properties determined with the Rheovibron are material dependent. Clearly then, these effects cannot be described sufficiently by a mechanical model analogue that accounts for the material response with a invariant dynamic spring constant. What needs to be described quantitatively is how the material response may be influenced by the conditions imposed on the sample during testing with the Rheovibron.

MODELLING MATERIAL RESPONSE

The dependence of the dynamic mechanical properties of a given polymer on the conditions imposed by the instrument and the sample dimensions necessitate a quantitative description of how these factors can influence the measured properties. In the following sections these effects are discussed along with quantitative methods by which material parameters that are independent of sample geometry and experimental conditions can be obtained.

Uniformity of imposed stress

During the performance of an extensional mechanical experiment, consideration must always be given to Saint-Venant's principle[23] which states that an irregular stress

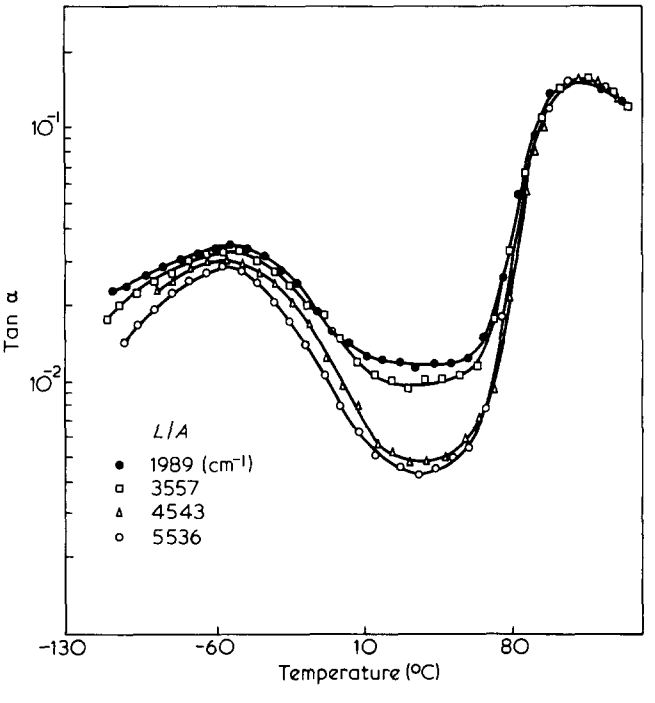

Figure 7 Measured tan α for PET at 11 Hz as a function of temperature and sample geometry (*L/A*)

distribution will arise in the sample as a result of transferring an external stress, via clamping, to the sample. This stress will become uniform at some characteristic distance from its point of application (i.e. the clamp). The principle further implies that the irregular stress distribution decays exponentially with distance, becoming negligible at about one sample width from the clamped end. In practice a sample aspect ratio (i.e. length/width) of 10 is sufficient for isotropic materials to ensure that a uniform stress exists throughout the sample[24]. For anisotropic materials detailed studies[24,25] have shown that the decay length, λ, can be expressed by the following relationship:

$$\lambda = b\left(\frac{E}{G}\right)^{1/2} \tag{15}$$

where b is the sample width, E and G are the tensile and shear moduli, respectively, in the test direction. Although, a minimum of 2λ is theoretically required to ensure a uniform stress distribution, we have found that 6λ to 8λ is usually necessary in dynamic mechanical experiments. Because the equations used to calculate the complex modulus or compliance assume a uniform stress distribution throughout the sample, it is essential that the aspect ratio criterion is met. If it is not met, the measured properties will deviate significantly from the true material properties. It has been demonstrated with different mechanical experiments, both in shear and tension, that the measured moduli approach asymptotically a constant value with increasing sample aspect ratio[24,26]. Furthermore, a simple empirical approach, in which the measured compliance was linearly extrapolated to zero reciprocal length, $(1/L)$, was demonstrated to yield a sample compliance that was independent of clamping effects[26]. In this work and in previous studies[10-12,17-21] sample dimensions were appropriately chosen so that geometry-independent material properties were measured. Finally, it is important to recognize that the Saint-Venant's principle places a constraint on the minimum sample length that can be used when determining the error constant, D_0, of the material with the Rheovibron (see equations 7 and 10).

Non-linear stress–strain behaviour

The dynamic mechanical properties of a polymeric sample may still exhibit a dependence on the sample dimensions even though the criterion of Saint-Venant's principle has been met. The Rheovibron is capable of operating at only a few discrete oscillating displacement amplitudes, and therefore if the sample length is changed from one measurement to the next, the oscillating strain amplitude cannot generally be kept constant. Also, it was found that the magnitude of the static displacement applied to the sample during a measurement was primarily determined by the amplitude of the oscillating displacement. Thus, for a fixed oscillating displacement, the static displacement required by normal balancing techniques[14], remained approximately constant irrespective of sample length. Therefore the use of different length samples will, in general, result in different operating strain and/or stress conditions during a measurement. Specifically, the magnitude of both the applied static strain and the oscillating strain amplitude are inversely proportional to the sample length used when the oscillating displacement amplitude is kept constant.

The Rheovibron manual[14] shows that the measured properties may show a dependence on the amplitude of the oscillating strain imposed on the sample during testing. Furthermore, previous investigators have also observed a similar dependence on the magnitude of the static strain which must be imposed on the sample during measurement[10-12,16,27]. It is clear that these observations imply a non-linear sample deformation response to measurement conditions. Consequently, in this work a quantitative modification accounting for this non-linear sample behaviour has been applied to Massa's treatment which modelled the material response by a linear spring constant.

The non-linear viscoelastic sample response was modelled following a procedure proposed by Mason[27,28]. Mason described the effect of the applied static strain on the measured dynamic mechanical properties of a rubber filament, by extending a Mooney–Rivlin representation for the sample's static or equilibrium non-linear stress–strain behaviour to dynamic conditions. Mason showed that the dependence of dynamic mechanical properties on the imposed static strain, was qualitatively similar to the behaviour observed for the static (i.e. equilibrium) properties. Thus a model which describes the dependence of a material's modulus and/or compliance on the applied static strain at equilibrium may also provide a reasonable description for the dependence of the dynamic properties on the applied static strain. A variety of models that attempt to describe non-linear stress–strain behaviour have been proposed[29,30]. However, most of these models require the determination of several experimental constants, and do not lend themselves to a simple descriptive analysis of dynamic mechanical data. A simple model is developed below to describe the non-linear stress–strain response in terms of parameters that can be experimentally determined with the Rheovibron.

In general, the stress–strain behaviour of an elastic or viscoelastic material can be expressed as an infinite power series expansion in stress, strain and/or stress and strain rates[31]. For small deviations from linearity, a truncated version of any of the above infinite series may adequately describe the material's behaviour. For example, the material's non-linearity under the equilibrium uniaxial tensile loading conditions imposed by the Rheovibron, can be described by the following simple, two-parameter equation:

$$\varepsilon = U_1\sigma + U_2\sigma^2 + \ldots \tag{16}$$

where σ and ε are the stress and strain, respectively, U_1 is the zero stress compliance and U_2 is a non-linear term that accounts for deviations from linearity.

A similar description of the non-linearity can be expressed as an infinite series in strain viz.

$$\sigma = C_1\varepsilon + C_2\varepsilon^2 + C_3\varepsilon^3 + \ldots \tag{17}$$

Although this equation can be used to describe the stress response of the material as a function of the imposed strain, it should be noted that equation (17) has no theoretical justification for a uniaxial tensile experiment. With reference to anisotropic elasticity theory[32], in a simple tensile experiment in which a uniaxial extension is

imposed on the material, the resulting tensile stress will be a function not only of the strain that has been applied along the deformation axis of the material, but also of the strains in the other two directions (i.e. lateral contractual strains). Consequently, if ε in equation (17) denotes only the extensional strain imposed on the material, then the parameters C_1, C_2, C_3 in equation (17) must depend on the lateral strains if the resulting tensile stress, σ, is to be described by this equation. Clearly, for a general description of the behaviour in a uniaxial tensile experiment, equation (17) cannot be rigorously applied. In contrast, equation (16) is ideally suited to describe the behaviour in a uniaxial tensile experiment, since only the stress along the deformation axis of the material is sufficient to describe the corresponding extensional strain[32]. By definition, the material compliance can be directly determined, in a general fashion, for a uniaxial tensile experiment, from the slope of the stress–strain response described by equation (16) (i.e. $S = d\varepsilon/d\sigma$). For an equilibrium or static experiment then, the modulus can be calculated by a simple inversion of the compliance, while in dynamic experiments the conversion of the compliance to modulus can be accomplished with equation (14).

In addition to the theoretical justification for modelling the deformation behaviour in terms of the applied stress, it should also be remembered that the Rheovibron which performs a uniaxial tensile experiment can be modified to provide a direct measure of the static force applied on the sample during a measurement. Furthermore, the amplitude of the oscillating force is obtained directly in terms of instrument parameters (see equation 5). These force readings are easily converted to the static stress and oscillating stress amplitude, if the cross-sectional area of the sample is known. Also, due to the series arrangement (see *Figure 5*) the sample and the instrument components are all under the same operating force. In contrast, the displacements that the sample and each component experience are different, and cannot be determined directly. However, once the spring constants of the various components are determined, their displacements can be calculated from a direct measurement of the operating force. The displacement of the sample within and between the clamps can then be determined, as the difference between the total system displacement and the displacement experienced by the instrument components. From the displacement calculated for the sample within and between the clamps and a measurement of the unstrained sample length, the strain for the sample between the clamps can be approximated.

In view of the foregoing discussions, it is both theoretically appropriate and experimentally easier to model the non-linear stress–strain response in terms of stress. Thus for the simple two-parameter form in stress provided by equation (16) the compliance in an equilibrium tensile experiment may be simply calculated by:

$$S = \frac{d\varepsilon}{d\sigma} = U_1 + 2U_2\sigma \tag{18}$$

with

$$E = S^{-1} \tag{19}$$

Equation (18), which is applicable to the equilibrium compliance, may be extended by Mason's procedure[27,28] to the dynamic compliance measured with the Rheovibron. This simple extension allows for storage (S') and loss (S'') compliances to be calculated as a function of the static stress, σ_{st}, that is applied in the dynamic experiment:

$$S' = U'_1 + 2U'_2\sigma_{st} \tag{20a}$$

$$S'' = U''_1 + 2U''_2\sigma_{st} \tag{20b}$$

The storage and loss compliances can be rearranged, along with equation (13), to give the complex compliance S^* for the experimental conditions applied during the measurement:

$$S^* = U^*_1 + 2U^*_2\sigma_{st} \tag{21a}$$

where

$$U^*_1 = U'_1 - iU''_1 \tag{21b}$$

$$U^*_2 = U'_2 - iU''_2 \tag{21c}$$

In equations (21), it should be recognized that U^*_1 is the zero stress complex compliance and U^*_2 is a non-linear complex compliance term. The real and imaginary components of these material descriptors (i.e. U'_1, U'_2, U''_1, and U''_2) are all functions of the temperature and rate of experimentation. The dependence of these parameters on the rate of experimentation will be addressed in a later section.

An inherent assumption in Mason's approach that has also been carried over in the present development, is that the oscillating stress response will be linearly related to the applied oscillating strain, irrespective of the degree of non-linearity that may be exhibited by the sample under the imposed static stress. It is interesting to note, however, that experimentally the Rheovibron cannot be balanced to perform a dynamic measurement on a sample unless the magnitude of the measured oscillating force response can be averaged by the instrument to appear linearly related to the magnitude of the imposed oscillating displacement. Thus even for a sample that may exhibit a high degree of non-linearity as a result of a large applied static deformation or large applied oscillating displacement amplitude, the Rheovibron will provide an averaged force response. The magnitude of the averaged force response will change with slight changes in the imposed conditions (i.e. with the static deformation or displacement amplitude). As a result of this averaging in the force response, the validity of Mason's assumption of linearity will always be satisfied as long as a measurement with the Rheovibron can be made.urthermore, this condition also allows for direct application of Massa's model to the dynamic mechanical data of a sample that have been measured with the Rheovibron at a given level of static deformation and oscillating displacement amplitude. Thus the influence of the instrumental components on the measured dynamic mechanical properties can still be taken into account.

It should be noted that equations (18), (20), and (21) represent only one of many models which may be used in describing the influence of non-linear sample behaviour on the measured dynamic mechanical properties. However, it is strongly suggested that if another model is developed, it should incorporate the experimental and theoretical considerations presented here. In summary, the present model was employed due to its generality, simple form and the ease by which the measured static stress is incorporated into the formulation. In the dis-

cussion that follows, this model will be used to illustrate a procedure that accounts for the influence of non-linear sample behaviour on the measured dynamic mechanical properties.

MODEL APPLICATION AND DISCUSSION

The model was evaluated using polyimide, polyethylene, polypropylene, poly(ethylene terephthalate) and other materials. This evaluation was carried out in two parts. First the static or equilibrium non-linear sample behaviour was investigated, which in part entailed the determination of the static stress–strain profile for the sample both within and between the clamps. To illustrate this analysis, the results for polyimide at 20°C are presented and discussed. Secondly, the dynamic mechanical response was investigated. This involved determining the dependence of the dynamic mechanical properties on the imposed static stress and the rate of experimentation. Results for polyimide and other materials, obtained at 11 and 110 Hz are presented and discussed. Also, as an illustration of the applicability of the model, the results from a complete analysis of polyimide at 110 Hz and 20°C are presented.

Static analysis

The Rheovibron was represented mechanically by a series of springs as shown in *Figure 5b*. The sample both within (i.e. clamped) and between (i.e. unclamped) the clamps was represented by a single static spring constant K_{st}. The spring constants for each of the instrument components, shown in *Figure 5b*, were determined as follows: The spring constants for the carbon steel rods and phenolic couples were calculated using the simple relation:

$$K = \frac{EA}{L} \tag{22}$$

along with geometrical dimensions (A/L) and literature values for the modulus, E[33,34]. The spring constant for the T1 stress gauge was calculated from the specifications provided by the Rheovibron instruction manual[14]. The driver spring constant was determined experimentally, by measuring its displacement as a function of the applied force. The force response of the driver was found to become non-linear at applied force levels greater than 4×10^5 dynes, a response attributed to the diaphragm-type driver design. Erroneous results caused by the driver non-linearity, were eliminated by operating only at stress levels where the driver response was linear. The values calculated for the spring constants associated with the various instrument components, are provided in *Table 1*. The spring constant for the driver is provided as a second degree polynomial in displacement. The coefficients for this polynomial were determined by least squares regression.

The total displacement experienced by the sample and the Rheovibron components was measured using a built-in Vernier caliper. Assuming a series addition, this total displacement was expressed as the sum of each component's displacement:

$$\Delta L_{total} = \Delta L_s + \Delta L_c + \Delta L_{T1\,gauge} + \Delta L_{driver} + \Delta L_{5\,cm\,rod} + 2\Delta L_{couple} + 2\Delta L_{2\,cm\,rod} + 2\Delta L_{8.5\,cm\,rod} \tag{23}$$

where ΔL_c and ΔL_s are the displacements experienced by the clamped and unclamped sample, respectively. The displacements, ΔL, that correspond to other instrument components are explicitly labelled. As shown in equation (23), the combined displacement of both the clamped and unclamped sample, is equal to the difference between the total displacement and the combined displacement of the instrument components. This displacement can be written in terms of the spring constants for each of the instrument components and the applied static force, F_{st}, as follows:

$$\Delta L_s + \Delta L_c = \Delta L_{total} - F_{st}\left(\frac{1}{K_{T1}} + \frac{2}{K_{R2}} + \frac{1}{K_{R5}} + \frac{2}{K_{R8.5}} + \frac{1}{K_D} + \frac{2}{K_C}\right) \tag{24}$$

From equation (24), the combined displacement for the clamped and unclamped sample can be calculated, by substituting appropriate values for the spring constants (see *Table 1*) along with the measured values for the total displacement ΔL_{total} and the applied static force F_{st}.

The strain for the unclamped part of the sample was defined as:

$$\varepsilon_s = \Delta L_s / L_s \tag{25}$$

where L_s is the unstrained length for the unclamped part of the sample. The strain experienced by the clamped part of the sample was defined as:

$$\varepsilon_c = \Delta L_c / L_c \tag{26}$$

where L_c is the unstrained length for the clamped part of the sample. Using equations (25) and (26) the combined displacement for the sample within and between the clamps can be written as:

$$\Delta L_s + \Delta L_c = \varepsilon_s L_s + \varepsilon_c L_c \tag{27}$$

The stress–strain behaviour for the sample between the clamps was described in terms of the series expansion in static stress:

$$\varepsilon_s = U_1 \sigma_{st} + U_2 \sigma_{st}^2 + \ldots \tag{28}$$

where U_1 and U_2 were previously defined (see equation 16). Similarly, the stress–strain behaviour for the sample within the clamps was also described in terms of the series expansion in static stress:

$$\varepsilon_c = I_1 \sigma_{st} + I_2 \sigma_{st}^2 + \ldots \tag{29}$$

where I_1 and I_2 are defined as a pseudo-zero stress compliance and a pseudo-non-linear compliance term for

Table 1 Spring constants for the rheovibron components

Component	Symbol	Value (dynes cm^{-1})
Stress gauge	K_{T1}	1.35×10^8
Phenolic couples	K_C	4.75×10^{10}
2 cm Rods	K_{R_2}	3.16×10^{10}
5 cm Rod	K_{R_5}	1.26×10^{10}
8.5 cm Rods	$K_{R_{8.5}}$	7.44×10^9
Driver	K_D	$2.99 \times 10^7 + 1.045 \times 10^9\,\Delta X - 1.126 \times 10^{11}\,\Delta X^2$

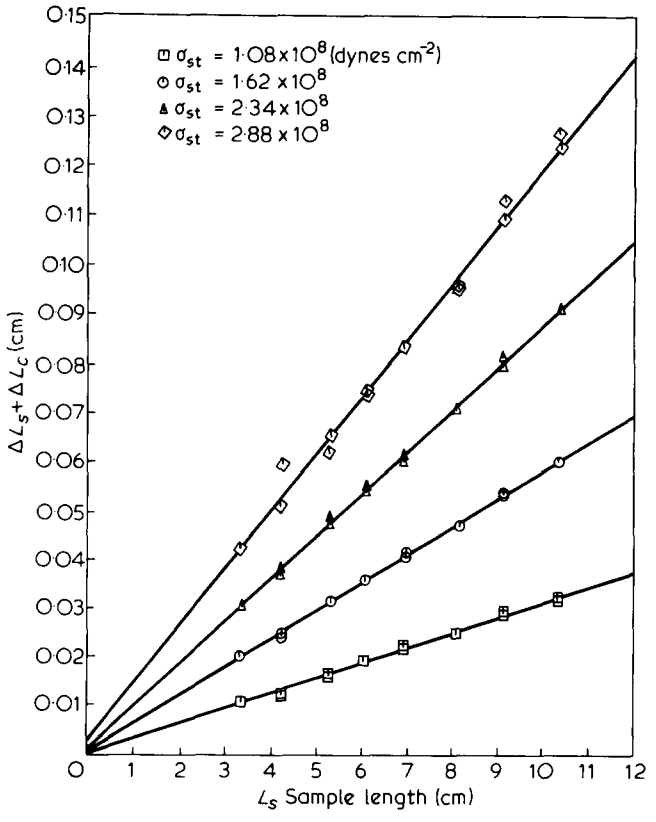

Figure 8 Sum of the displacements within and between the clamps, $\Delta L_s + \Delta L_c$, for polyimide at 20°C, are provided as a function of the unstrained sample length for the sample between the clamps L_s, at fixed levels of applied static stress

the material within the clamps, respectively. The compliance properties assigned to the sample within the clamps were termed *pseudo*, since they were calculated on the assumption of a pure tension mode, although the real stress distribution within the clamps is a complicated combination of tension, shear and compression[32].

Equations (28) and (29) state that at a fixed static stress, the strains experienced by the clamped and unclamped sample are constant, irrespective of the sample length. Thus, if the length of sample within the clamps and the applied static stress are kept constant, the combined displacements for the clamped and unclamped part of the sample will vary linearly with the unclamped sample length (see equation 27). The slope of this line will be equal to ε_s, and the intercept will provide the product of L_c and ε_c. With our new clamp design, for a properly trimmed sample, the length of the sample within the clamps is equal to the clamp length. Since the length of the clamps used in this study was 0.4 cm, the total length of the sample within the clamps was always equal to 0.8 cm. In *Figure 8*, the combined displacement for the clamped and unclamped part of a polyimide sample at 20°C is plotted for four different static stress levels. The observed linear dependence on the unclamped length of the sample, is consistent with the expected behaviour. Data taken at other stress levels also showed the same dependence on the unclamped length of the sample but are not plotted in *Figure 8* for reasons of clarity. In *Figure 9*, all the data are plotted as static stress–strain curves for both the material within and between the clamps. The lines drawn are the best fits obtained using both second and third order forms of equations (28) and (29). The material descriptors determined are given in *Table 2*. As can be seen from *Figure 9*, the non-linearity of the unclamped part of the sample was adequately described by the second order form of equation (28). In contrast, a third order form of equation (29) was required adequately to describe the non-linear stress–strain behaviour observed for the material within the clamps. Although the extent of the non-linear stress–strain behaviours observed for the clamped and unclamped sample were different, it is interesting to note that their responses became non-linear at approximately the same static stress level.

As discussed above, static analysis provides a procedure for the determination of the static strain imposed on the unclamped part of the sample during a measurement. However, this procedure is complicated by the fact that the displacement experienced by the clamped and

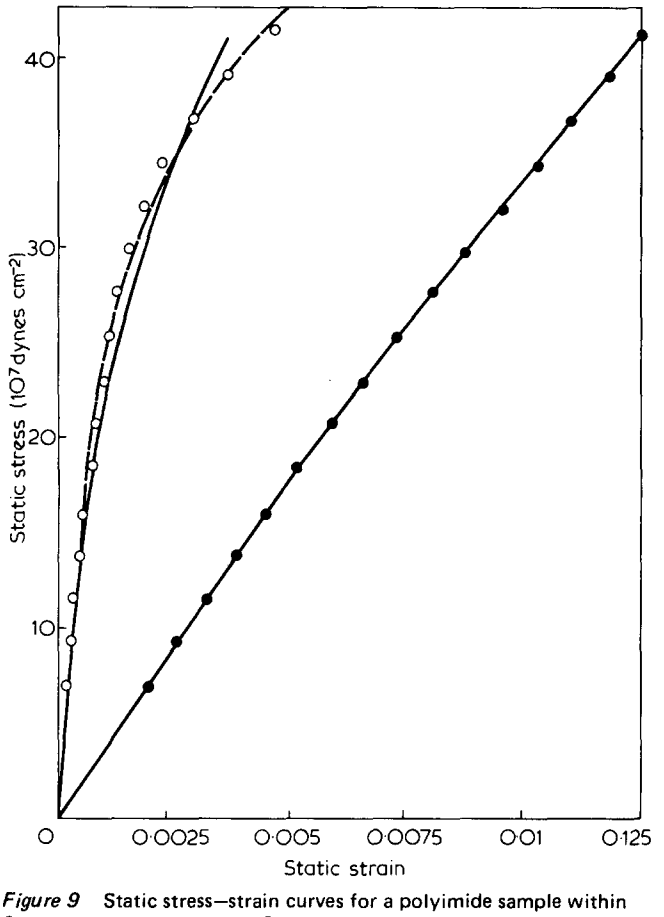

Figure 9 Static stress–strain curves for a polyimide sample within ○; and between the clamps, ●. The lines drawn were determined by regression analysis, using second, ——; and third order forms, – – –; of equations 28 and 29

Table 2 Material descriptors for polyimide at 20°C from static analysis

(a) Descriptors for the sample between the clamps	
U_1 x 10^{11} [cm^2 dyne^{-1}]	U_2 x 10^{21} [cm^2 dyne^{-1}]^2
2.7 ± 0.025	7.63 ± 0.93

(b) Descriptors for the sample within the clamps		
I_1 x 10^{12} [cm^2 dyne^{-1}]	I_2 x 10^{20} [cm^2 dyne^{-1}]^2	I_3 x 10^{29} [cm^2 dyne^{-1}]^3
0.45 ± 0.72	1.96 ± 0.27	–
4.83 ± 0.71	−2.52 ± 0.66	9.23 ± 1.3

unclamped parts of the sample must be separated into their respective components. Although this analysis can be simplified for long samples, where ΔL_c will become small compared with ΔL_s, allowing ε_s to be approximated by:

$$\varepsilon_s = \frac{\Delta L_s + \Delta L_c}{L_s} \tag{30}$$

It can be seen from *Figure 8* that for a 5 cm polyimide sample at 20°C, use of this approximation would result in overestimating ε_s by about 5%. The size of this error will depend on the polymer used, its dimensions and the temperature of experimentation. Furthermore, measurement of the imposed static strain requires measurement of the applied static force, from which the static stress can be directly calculated if the cross-sectional area is known. This result further emphasizes the advantage of modelling the non-linear response in terms of stress.

In summary, it was shown that equations (28) and (29) can describe the non-linear equilibrium stress–strain behaviour observed for polyimide at 20°C. The fact that the response within the clamps and the response between the clamps could be described by similar equations implies that clamping effects can be accounted for by modelling an effective tensile stress–strain behaviour for the sample within the clamps.

DYNAMIC ANALYSIS

Experimental conditions

In the static analysis section it was shown that the influence of the sample's non-linear stress–strain response on the measured equilibrium properties could be completely characterized by the magnitude of the applied static stress. In contrast, characterization of the test conditions during a dynamic experiment requires that the experimental rate also be specified. According to classical linear viscoelasticity theory[31], the experimental rate for a dynamic mechanical test is completely characterized by the frequency of the applied sinusoidal displacement and/or force. However, as discussed previously, due to non-linearities in the sample's viscoelastic response, the measured dynamic mechanical properties may also show a dependence on the magnitude of the applied oscillating displacement or force. Therefore, a concise characterization of the test conditions imposed during a dynamic experiment requires that the static stress, frequency and magnitude of the applied oscillating displacement or force must all be specified. By analogy to classical stress–strain experiments which are performed at either a fixed stress or strain rate, it was convenient also to define the dynamic experimental rate in terms of stress and strain.

During a dynamic experiment the stress applied to the sample is composed of both a static and a dynamic (i.e. time-dependent) part, denoted as σ_{st} and σ_{dyn}, respectively. The components of the applied stress may be defined as:

$$\sigma_{st} = \frac{F_{st}}{A} \tag{31a}$$

$$\sigma_{dyn} = \frac{F_o}{A} e^{i(\omega t + \alpha)} = \sigma_o e^{i(\omega t + \alpha)} \tag{31b}$$

where σ_o is the oscillating stress amplitude. The total operating stress applied to the sample is given by the sum of the static and dynamic components:

$$\sigma(t) = \sigma_{st} + \sigma_o e^{i(\omega t + \alpha)} \tag{32}$$

from which the experimental stress rate, $\dot{\sigma}$, can be easily calculated:

$$\dot{\sigma} = \frac{d\sigma(t)}{dt} = i\omega\sigma_o e^{i(\omega t + \alpha)} \tag{33}$$

Using the root-mean-square (r.m.s.) value, the stress rate can be expressed as:

$$\dot{\sigma} = 0.707\ \omega\sigma_o \tag{34}$$

Consequently the stress rate is proportional to both the angular frequency, ω, and the amplitude of the oscillating stress, σ_o. Therefore the rate of experimentation is not completely described by specifying only the frequency of the experiment. This result also implies that equivalent stress rates can be obtained while operating at different frequencies by varying the amplitude of the applied oscillating stress. However, operation at equivalent stress rates does not necessarily imply that equivalent dynamic mechanical properties will be measured, since as the amplitude of the applied oscillating stress is increased structural changes in the sample and therefore the measured properties may result. Any two of the three parameters (i.e. frequency, stress rate and the amplitude of the oscillating stress) are sufficient to characterize the dynamic response. Here, the static stress, frequency, and stress rate were chosen to describe the experimental conditions imposed on the sample during measurements with the Rheovibron.

By analogy a similar expression can be written for the strain rate, $\dot{\varepsilon}$, applied to the sample:

$$\dot{\varepsilon} = 0.707\frac{X_o^u}{L_{un}} = 0.707\ \omega\varepsilon_o \tag{35}$$

where X_o^u is the oscillating displacement experienced by the unclamped sample only, and ε_o is the oscillating strain amplitude. The strain rate may be related to the stress rate through the complex compliance:

$$\dot{\varepsilon} = |S^*|\dot{\sigma} \tag{36}$$

allowing them to be used interchangeably.

Experimentally the stress rate is easier to determine than the strain rate, since it can be calculated directly from the measured dynamic force, the sample's cross-sectional area and the angular frequency. In contrast, the determination of the strain rate requires a separation into a clamped and unclamped part similar to that discussed in the static analysis section. Neither the stress rate nor the strain rate can, in general, be kept constant when different dimension samples are used since the Rheovibron's design only allows for operation at a few discrete oscillating displacement amplitudes. This problem can be resolved by modifying the Rheovibron to operate at preselected oscillating force levels, which can be adjusted continuously to allow the stress rate to be kept constant when different geometry samples are used.

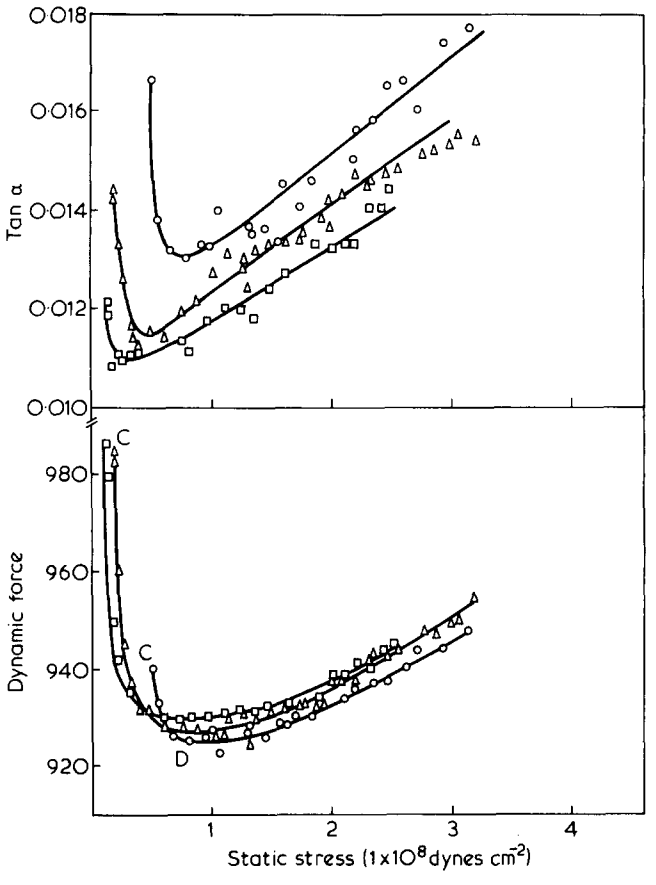

Figure 10 Dependence of the measured loss tangent and dynamic force on the applied static stress and the stress rate, for polyimide at 11 Hz and 20°C. The stress rate ranges were: □, 1.5–1.6; △, 4.7–4.9; and ○, 14.8–15.5; in units of 10^8 dynes cm^{-2} s^{-1}. The points D and C designate the static stress levels balanced at and the properties measured using balance procedures one and two, respectively

To investigate the dependence of the measured properties on the applied static stress and stress rate, measurements were made at different oscillation amplitudes, and at various static stress levels. The range of static stress levels at which measurements can be made is bounded for given sample dimensions. The minimum static stress which can be used is determined by the size of the applied oscillating displacement which is just sufficient to prevent buckling. The maximum static stress which can be used, is determined by either the upper limit of the driver's linear response, sample fracture, or by the point where the sample's non-linearity is so great that stable instrument balance cannot be obtained. In *Figure 10*, tan α and the product of $D(AF)$ for polyimide at 20°C are both given as a function of the applied static stress at three diferent stress rates. The operating frequency for all of these measurements was 11 Hz, and the stress rate was varied by operating at the three different discrete oscillating amplitudes (i.e. 0.0016, 0.05, and 0.16 cm). In these experiments, as well as all other experiments with polyimide at 20°C, the maximum static stress level used was determined by the onset of the driver's non-linear behaviour. For the results presented in *Figure 10*, the maximum static stress level used corresponded to operation at a static strain of approximately 1.25% for the sample between the clamps. Both tan α and the product $D(AF)$ were found to decrease initially with increasing static stress and then gradually increase with further increases in the applied static stress. An increase in the stress rate resulted in increasing the measured tan α at all the static stress levels investigated. In contrast, increasing the stress rate resulted in an increased $D(AF)$ value being measured for the static stress levels up to approximately 7×10^7 dyne cm^{-2}. At larger static stress levels the opposite trend was observed. The large dependence observed for tan α and $D(AF)$ on the static stress and the stress rate, emphasize the importance of both controlling and specifying the experimental conditions under which the measurement is made.

In addition to the experimental conditions discussed, consideration must also be given to the effect of stress relaxation on the measured dynamic properties. For the low stress and/or strain levels typically used with the Rheovibron, the dependence of the dynamic mechanical properties on time was found to be negligible for the materials examined in this study. This result is consistent with the data for polycarbonate reported by Litt[16], which showed a decreased dependence of E' and E'' on time as the level of the applied static strain was decreased.

The possibility that the static stress levels imposed on the sample could have altered the material structure irreversibly was investigated by the following experiment. Measurements were made at various static stress levels, which were increased stepwise from the minimum to the maximum level and then decreased stepwise back to the minimum level. If no hysteresis was observed in the dynamic mechanical properties, the sample's structure was be assumed to remain unchanged. For polyimide at 20°C, even after repeating this procedure five times, no hysteresis was observed in the dynamic mechanical properties measured.

Instrument balance

As discussed in the previous sections and in other studies[15–21,27,28] the dynamic mechanical properties measured with the Rheovibron can show a large dependence on the magnitude of the static stress or strain imposed on the sample during a measurement. Two different procedures for determining the proper static stress or strain are given in the Rheovibron instruction manual[14]. A detailed investigation of these balancing methods showed that they did not always result in balancing at the same static stress level. Furthermore, it was found that balancing at these different static stress levels could result in measured properties which differed by as much as 30–50%.

The first procedure for instrument balance involves monitoring the tan α-meter deflection, while operating in the dynamic force position of the main selector switch, as strain or tension is applied to the sample. As described in the instruction manual[14], the proper strain or tension level is indicated by an inflection point in the meter deflection *versus* strain or tension curve. As shown schematically in *Figure 11a*, the meter deflection profile as a function of the applied strain or tension varies for different materials. These differences often make the determination of the inflection point, P, difficult. This difficulty may be particularly encountered for a material whose response is represented by line C in *Figure 11a*. Though these different types of responses were discussed in the instruction manual no explanation of their cause was given. The first balance procedure corresponds to

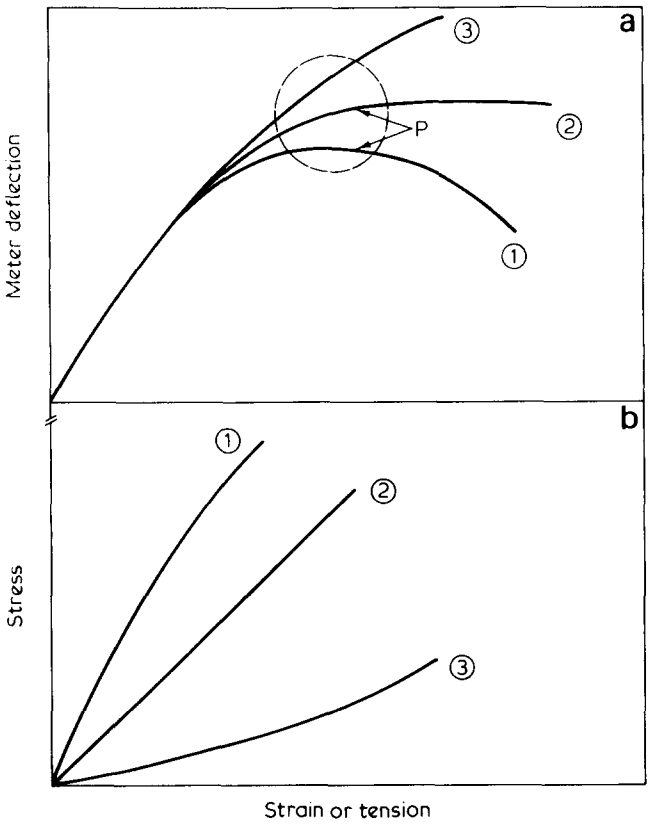

Figure 11 (a) Possible tan δ meter deflection responses, to the applied strain or tension, that may be observed for different samples. The correct balance point is indicated by point P. (b) The stress–strain behaviour which corresponds to the different meter deflection profiles given in *Figure 11a*

balancing at point D in *Figure 12* where the sinusoidal stress response for a fixed oscillating displacement is schematically given for operation at various static stress levels. Furthermore, use of this balance procedure resulted in measurement of the properties at the static stress levels denoted by point D in *Figure 10*.

The second balancing procedure involves observing the resulting oscilloscope Lissajous figure, while operating in the dynamic force setting of the main selector switch. When the sample slightly buckles, as at point B in *Figure 12*, the oscilloscope Lissajous figure is a diagonal line with a small loop or break at one end. As strain or tension is applied to the sample, this loop or break is removed. At the point where this loop or break has just been removed, the sample no longer buckles and a measurement can be made. This procedure resulted in balancing at point C in *Figure 12* which also corresponded to measurements of the properties denoted by point C in *Figure 10*.

The large difference in the properties measured by using these two balance procedures is evident and may be partly responsible for the data variation observed between different operators and studies that have appeared in the literature. The second procedure at first appeared to be the better of the two methods, because it resulted in operating at a static stress level just greater than the minimum required to prevent the sample from buckling. However, further analysis of the above results led to the conclusion that the first balancing procedure, which consisted of monitoring the tan δ-meter deflection as a function of the applied strain or tension was correct. In support of this conclusion the following observations in experiments with polyimide are presented: Since the dynamic force to a first approximation is inversely proportional to the material's complex modulus, the large decrease in $D(AF)$ observed in changing from balance point C to D in *Figure 10* suggests a dramatic increase in the material's modulus for an extremely small change in the applied static stress. Secondly, the minimum observed in the $D(AF)$ *versus* static–stress curve implies an abrupt maximum in the material's modulus. Neither of these observations are consistent with the static stress–strain curve presented in *Figure 9*, nor with stress–strain data obtained using an Instron tester. However, the gradual increase of $D(AF)$ with increases static stress, for static stress levels which are greater than those which correspond to point D in *Figure 10*, suggests a slight non-linearity consistent with the stress–strain behaviour observed for polyimide. In summary, it is of extreme importance that Rheovibron operators be aware of the large differences that may exist in the properties measured, as a result of the two balancing procedures (see *Figures 10* and *12*). In addition, these results further illustrate the importance of monitoring the static stress applied during a measurement.

For comparison, 20°C data for polypropylene taken at two stress rates and at various static stress levels are given in *Figure 13*. In contrast to the behaviour observed for polyimide, where the maximum static stress used was determined by the upper limit of the driver's linear response, the maximum static stress used in the experiments with polypropylene was determined by the higher degree of the sample's non-linearity. This non-linearity resulted in unstable instrument balance, which prevented measurements at higher static stress levels from being made. For polypropylene at 20°C the maximum static force used was 1.5×10^5 dynes, as compared with 4×10^5 dynes for polyimide at 20°C. The stress rate used in the experiments with polypropylene, was varied by operating at 11 and 110 Hz, with an oscillating displacement amplitude of 0.005 cm. As in the case of polyimide both tan α and $D(AF)$ initially decreased and then increased

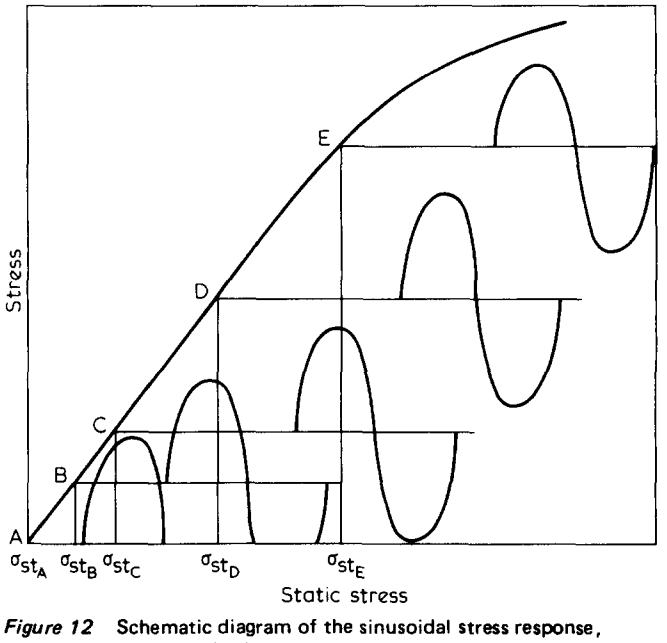

Figure 12 Schematic diagram of the sinusoidal stress response, for a fixed oscillating displacement, at various static stress levels

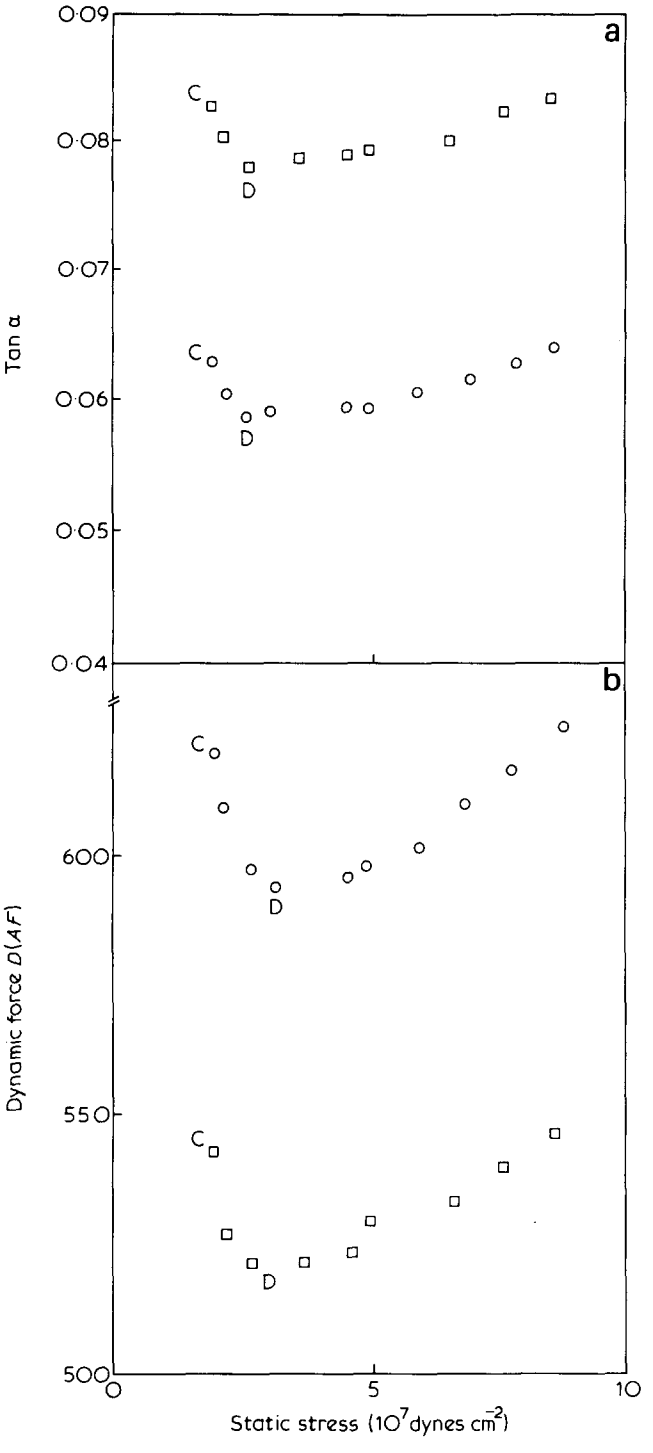

Figure 13 Dependence of the measured loss tangent (a) (tan α); and (b) dynamic force (*DF*) on the applied static stress and stress rate, for polypropylene at 20°C. The ranges of stress rates used were: ○, 4.5–4.7 x 10^8; and □, 5.1–5.5 x 10^9; in units of dynes cm^{-2} s^{-1}. These stress rates were achieved by operating at 11 and 110 Hz, respectively

with increasing static stress. The properties obtained for polypropylene, using balance procedures one and two are denoted by the points D and C, respectively. A close comparison of *Figures 10b* and *13b*, shows that the product $D(AF)$, at static stress levels greater than those obtained using balance procedure one, increased faster with increasing static stress for polypropylene than for polyimide. Since $1/D(AF)$, to a first approximation, is inversely proportional to the samples complex modulus, this difference was attributed to the higher degree of sample non-linearity in stress–strains that is observed for polypropylene.

For all the materials investigated, it was observed that the plots of meter deflection and $1/D(AF)$ *versus* the applied tension, obtained from the same sample under equivalent conditions, were qualitatively similar. For example, a plot of $1/D(AF)$ *versus* strain or tension for the polyimide data given in *Figure 10b*, corresponds to the meter deflection profile represented schematically by line 2 in *Figure 11a*. In contrast, a similar plot of $1/D(AF)$ for the polypropylene data provided in *Figure 13b*, corresponded to the meter deflection *versus* tension curve indicated by line 1 in *Figure 11a*. From these and similar results obtained for different materials, the meter deflection curves given in *Figure 11a* were associated with the corresponding stress–strain behaviour shown schematically in *Figure 11b*.

THE COMPLEX COMPLIANCE AND THE ERROR CONSTANT

In order to determine explicitly the complex compliance or modulus of a polymeric sample, and their dependence on the applied static stress and the stress rate, the error constant D_o must be determined. Upon rearrangement, equation (9a) can be written as follows:

$$D(AF)(1+W) = B|S^*|\frac{L}{A} + D_o = \frac{B}{|E^*|}\frac{L}{A} + D_o \quad (37a)$$

with

$$B = 2\times 10^9\left(1 - \frac{M\omega^2}{S_m^o}\right) \quad (37b)$$

$$W = \left(1+\left(\frac{D_{oc}}{D}\right)^2 - 2\left(\frac{D_{oc}}{D}\right)\cos\alpha\right)^{1/2} - \left(\frac{D-D_{oc}}{D}\right) \quad (37c)$$

where B and W are rearrangements of the correction factors for the effect of the instrument components on the measured properties that were discussed by Massa[1]. Equation (37a), implies that a plot of $D(AF)(1+W)$ as a function of the geometric parameter, L/A, would be linear. The slope of this line should be proportional to the complex compliance, and the intercept should be equal to the error constant D_o. However, before equation (37a) can be used the instrument's mass, M, and spring constant, S_m^o, must be evaluated. The instrument's mass M, was experimentally determined to be 6 grams by weighing the rods, couples and clamps. The instrument's spring constant S_m^o, was calculated by assuming a series arrangement of the components:

$$S_m^o = \frac{1}{\frac{2}{K_{R2}} + \frac{2}{K_{R8.5}} + \frac{1}{K_{T1}} + \frac{1}{K_C}} \quad (38)$$

which upon substitution of the appropriate spring constant values in *Table 1* gave $S_m^o = 1.35\times 10^8$ dyne cm^{-1}. It should be noted that in the dynamic case, following Massa's modelling approach, only the components between the T1 and T7 gauges are taken into account in equation (38) (see *Figure 5*). The calculated S_m^o value was substituted in equation (10b), which for an amplification factor of one ($AF = 1$) gave $D_{oc} = 14.8$. This value is significantly different from Massa's[1] experimentally de-

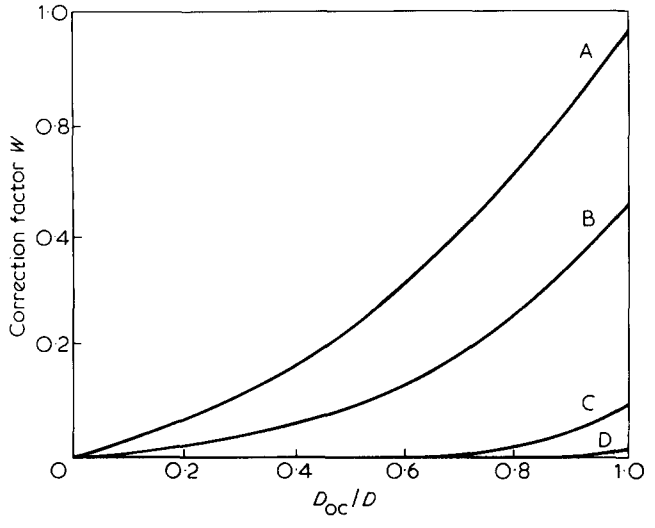

Figure 14 Correction factor (W), as a function of the dynamic force parameters (D_{OC}/D) for specific values of tan α: A, 0.01; B, 0.1; C, 0.5, and D, 1

termined value of 24.0, which corresponds to an instrument S_m^o value of 8.3×10^7 dynes cm^{-1}. This uncertainty of the correct value for D_{oc} or S_m^o, makes it impossible to calculate exact values for the parameters B and W used in equation (37a). Therefore, before the complex compliance or the error constant can be calculated, the constant component of the error constant, D_{oc}, must be determined. In the following discussion a procedure for the determination of D_{oc} is presented.

In *Figure 14*, the dependence of the correction factor W, on tan α and the ratio of D_{oc}/D is given. From this figure it is evident that the correction factor W, approaches zero as either tan α or D_{oc}/D approach zero. This implies that a sample from a given polymeric material can be chosen with appropriate dimensions so that the correction factor W, will be negligible. Thus equation (37a) can be used for the determination of the error constant D_o, without knowing D_{oc}. As shown in *Figure 14*, the value of the correction factor is $W < 0.01$ for a material whose measured loss tangent is tan $\alpha = 0.01$ for all values of D_{oc}/D. Therefore the assumption that the correction factor is equal to zero for a material with tan $\alpha = 0.01$ results in a maximum error of 1% when equation (37a) is used. Specifically, when tan $\alpha = 0.01$ and $D_{oc}/D = 0.5$ this error is only 0.005%. Furthermore, the estimated values for D_{oc}, (i.e. 14.8 and 24), suggest that the ratio D_{oc}/D will be less than 0.5 even when the material and sample dimensions used result in a dynamic force value as low as $D = 50$. Therefore, if a material with a loss tangent tan $\alpha = 0.01$ is used, the assumption that the correction factor W, is equal to zero will be valid. Thus for polyimide at 20°C, whose loss tangent was in the range $0.01 \leqslant \tan \alpha \leqslant 0.024$ depending on the applied static stress and stress rate, the assumption that the correction factor W is zero resulted in negligible errors when equation (37a) was applied to the data.

In the static analysis section it was shown that the stress–strain behaviour for the sample within the clamps could be described by a set of pseudo compliance parameters. Extension of this result to the dynamic case, suggests that the sample within the clamps can be represented by an effective complex compliance, $I^*_{o\,eff}$, which depends on both the static stress and the stress rate.

The magnitude of this effective complex compliance, $|I^*_{o|eff}$ can be related to the magnitude of the dynamic spring constant for the material within the clamps by combining equations (19) and (22).

$$|K^*_o| = \frac{1}{|I^*_{o|eff}} \frac{L_c}{A} \tag{39}$$

Substituting equations (37b) and (39) into equation (10) the error constant can be expressed as

$$D_o = B|I^*_{o|eff} \frac{L_c}{A} + D_{oc} \tag{40}$$

Equation (40) implies that the error constant, D_o, will vary linearly with the sample dimensions within the clamps, L_c/A. The slope of this line will be proportional to the magnitude of the effective complex compliance $|I^*_{o|eff}$ for the sample within the clamps, and its intercept will provide the constant component of the error constant D_{oc}. Since, with the new clamp design, the length of the sample within the clamps was always equal to twice the clamp length or $2L_c = 0.8$ cm, (see static analysis section), the geometric parameter L_c/A, will depend only on the sample's cross-sectional area. Thus experimental application of equation (37a) for the determination of a polymer's complex compliance and error constant, requires that the cross-sectional areas of the samples used be kept constant. This result also implies that the geometric parameter for the sample between the clamps L/A, should be varied only by changing the unstrained sample length, when equation (37a) is used.

The complex compliance and the error constant, at a given temperature and frequency, are both functions of the applied static stress and the stress rate. Thus these conditions must be kept constant as different geometry samples are used for the determination of $|S^*|$ and D_o (see equation (37a)). As discussed previously, the static stress can be varied continuously and therefore in most cases, can be kept constant irrespective of the sample geometry used. In contrast, the stress rate cannot be kept constant as different geometry samples are used, since the Rheovibron can be operated only at a few discrete oscillating amplitudes. Furthermore, the common practice is to use only one oscillating displacement amplitude as the sample geometry is changed. This practice will always result in increasing the amplitude of the oscillating stress and therefore the stress rate as the sample geometric parameter L/A, is decreased. As illustrated with polyimide at 20°C, the effect of operating at higher stress rates on the measured properties cannot be neglected (see *Figure 10*). Since the stress rate cannot be kept constant as the sample's geometry L/A is changed, the range of stress rates used for each experiment is reported for the results that are presented here.

The quantity $D(AF)$ was plotted against the geometric parameter L/A, at various static stress levels for a polyimide sample at 20°C. The values of the static stress used, ranged from 7×10^7 to 4.3×10^8 dynes cm^{-2}. In *Figure 15* the data obtained at the highest and lowest static stress values are provided. The cross-sectional area of the sample was 1.04×10^{-3} cm^2, and therefore the geometric parameter for the material within the clamps was $L_c/A = 765$ cm^{-1}. The frequency of experimentation was 110 Hz, while the oscillating displacement amplitude

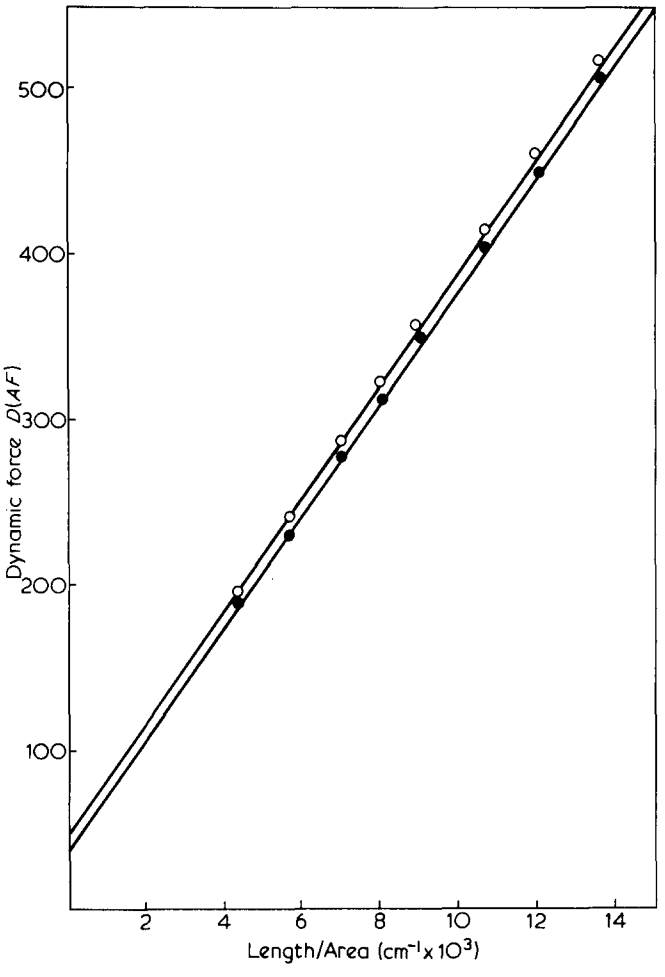

Figure 15 Product $D(AF)$ as a function of the sample's geometric parameter (L/A), at two different applied static stress levels; ●, 7.0 x 10^7 dynes cm^{-1} and ○, 4.3 x 10^8 dynes cm^{-1}; for polyimide at 20°C and 110 Hz. The range of stress rates used was 0.8–2.6 x 10^9 dynes cm^{-2} s^{-1}. The lines shown were determined by least squares regression of equation (37a)

was 0.005 cm. These conditions resulted in a range of stress rates, which increased from $8. \times 10^9$ to 2.6×10^{10} dynes cm^{-2} s^{-1}, as the sample length was decreased from 10.26 to 3.3 cm, respectively. To further investigate the effect of increasing stress rate on the measured properties, a different oscillating amplitude equal to 0.016 cm was also used for each sample length at the same static stress levels. Operating at this larger oscillation amplitude resulted in increasing the stress rate by approximately 3.1 times. The different oscillating amplitudes allowed for the determination of the effect of stress rate on the measured dynamic properties, while keeping the sample dimensions and the static stress constant. The data shown in *Figure 15*, along with additional data obtained at intermediate static stress levels, were fitted by least squares regression of equation (37a). The slope of these lines were found to increase slightly as the static stress was increased. This slight increase in slope corresponds to a slight increase in the complex compliance as the static stress is increased. This result is consistent with the behaviour observed for polyimide in the static analysis. In contrast, as is shown in *Figure 16*, the error constant, which is provided by the intercept of these lines, changed by approximately 15%, increasing from 39.0 to 46.0 over the range of static stress levels investigated. This large change in the error constant, with applied static stress, corresponds to the highly nonlinear response that was observed for the sample within the clamps in the static analysis section.

The procedure discussed above was repeated using five polyimide samples, each having a different cross-sectional area, A, at both 11 and 110 Hz and 20°C. Operation at the different frequencies corresponded to stress rates which ranged from $0.4–2.6 \times 10^9$ dynes cm^{-2} s for 11 Hz and $0.6–3.0 \times 10^{10}$ dynes cm^{-2} s for 110 Hz, respectively. In *Figure 17*, the error constants determined at a static stress level of 1×10^8 dynes cm^{-2} are plotted as a function of the geometric parameter L_c/A. The best fit lines obtained from linear regression of the data are also provided in *Figure 17*. Although the error constant was found to vary linearly with L_c/A, as predicted by equation (40), the intercepts obtained for the 11 and 110 Hz data were found to be 24 ± 3.4 and 14 ± 2.8 respectively, indicating a significant difference. Though similar plots at different static stress levels gave the same intercept values, the slopes of the lines obtained were different. Specifically, as the applied static stress was increased, the slope of these lines increased. According to equation (40) this result implies that the effective compliance for the material within the clamps increases as applied static stress was increased. This is consistent with the behaviour observed for the material within the clamps in the static case.

Also shown in *Figure 17*, are the results obtained at 20°C using a high density polyethylene sample. Since the measured loss tangent for this sample ranged in the interval $0.022 \leqslant \tan\alpha \leqslant 0.040$, depending on the static stress and the stress rate used during testing, it was assumed that $W \cong 0.0$. The polyethylene data were taken at a static stress level of $5. \times 10^8$ dynes cm^{-2}, at both 11 and 110 Hz. Operation at these frequencies resulted in stress rates of 0.4 to 1.1×10^9 dynes cm^{-2} s^{-1} for the 11 Hz and 0.45 to 1.15×10^{10} dynes cm^{-2} s^{-1} for the 110 Hz. The values for D_{oc} obtained with polyethylene at 11 and 110 Hz, were 27 ± 2.2 and 12.5 ± 2.5, respectively. These

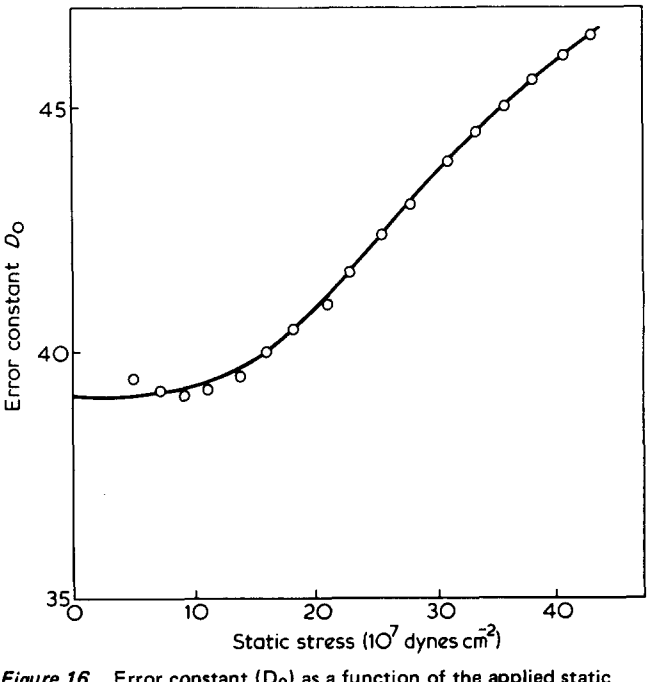

Figure 16 Error constant (D_0) as a function of the applied static stress for polyimide at 110 Hz and 20°C. The stress rates used ranged from 0.8–2.6 x 10^9 dynes cm^{-1} s^{-1}. Geometric parameter for the material within the clamps (L_c/A), was 765 cm^{-1}

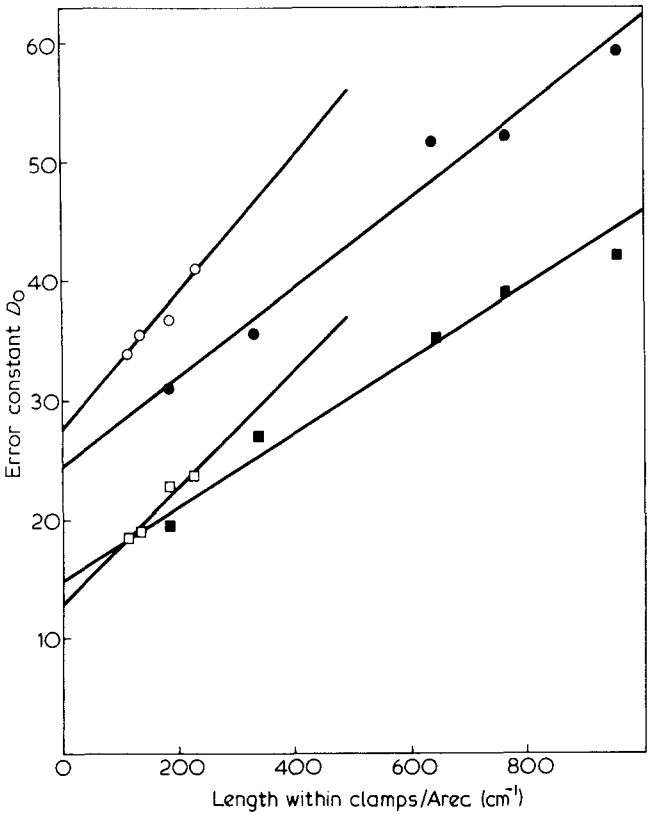

Figure 17 Error constant (D_0), determined for polyimide (●, ■) and polyethylene (○, □), at 20°C are plotted as a function of the geometric parameter (L/A). Data at both 11 Hz (○, ●) and 110 Hz (□, ■) are presented for these materials. The lines provided were determined by least square regression of equation (40). The intercepts of these lines provide an experimental measure of the constant component of the error constant D_0 at the given frequency

values of D_{oc} are in excellent agreement with the results obtained with the polyimide samples. The average values determined, for D_{oc}, from the results for polyimide, polyethylene, and other materials examined, are 14 ± 3 and 26 ± 3 at 110 and 11 Hz, respectively. The assumption that W was equal to zero, for all of the materials used in the determination of D_{oc}, was checked using the average values determined for D_{oc}. The maximum error in using equation (37a) was found to be less than 0.01%. Thus the validity of the assumption that $W \cong 0.0$ for all the polymers examined was independently tested, giving added confidence in the averaged D_{oc} values obtained. Although the averaged value for D_{oc} used in the compliance calculations was found to be independent of the applied static stress as expected, its dependence on the operating frequency used was unforseen. However, it is interesting to note that the 110 Hz D_{oc} value is in excellent agreement with the theoretically calculated value of 14.8. This result is consistent with the fact that the electronic calibration of the Rheovibron is done at 110 Hz[36] and suggests that the difference between the values obtained for D_{oc} at 11 and 110 Hz is due to the instruments amplification electronics. Although attempts were made to determine the exact cause of this difference, we were unable to provide a method or modification by which this discrepancy could be corrected.

The parameter B that was also calculated with the average values for D_{oc} and equations (10a) and (37b), assumed the values of 2×10^9 dynes cm^{-2} at 11 Hz and 1.96×10^9 dynes cm^{-2} for the 110 Hz frequency. Using these values for B, the complex compliance was calculated from the slope of equation (37a). In *Table 3* the complex compliance calculated for polyimide is given as a function of the static stress and the range of stress rates used.

In comparing the results obtained for different materials, it is useful to define the ratio of the effective complex compliance for the sample within the clamps and the complex compliance for the sample between the clamps as:

$$R = \frac{|I^*_{ole ff}}{|S^*|} \tag{41}$$

The ratio R, so defined will depend on the static stress, the stress rate, and the temperature of experimentation.

For polyimide at 20°C and 110 Hz, the magnitude of the effective complex compliance for the sample within the clamps, $|I^*_{ole ff}$, the complex compliance for the sample between the clamps, $|S^*|$, and R are plotted in *Figure 18* as a function of the applied static stress. For the range of static stress levels investigated, a linear dependance on the applied static stress was observed for $|S^*|$. This observation is consistent with the fact that a second order form of equation (28) was found to adequately describe the equilibrium stress–strain behaviour for the sample be-

Table 3 Complex compliance* for polyimide at 20°C as a function of the applied static stress and stress rate

Frequency [Hz]	Stress rate [x10^9 dynes cm^{-2} s^{-1}]	Static stress [σ_{st} x10^8 dynes cm^{-2}] 1.4	2.4	3.3	4.3
–	–	2.92	3.06	3.20	3.35
11	0.85–1.77	2.52	2.53	2.57	2.61
11	2.7–4.6	2.44	2.44	2.47	2.51
110	9.2–25.5	2.38	2.39	2.41	2.43
110	29.7–63.6	2.37	2.39	2.40	2.41

* In units of [$|S^*|$ x10^{11} cm^2 dyne^{-1}]

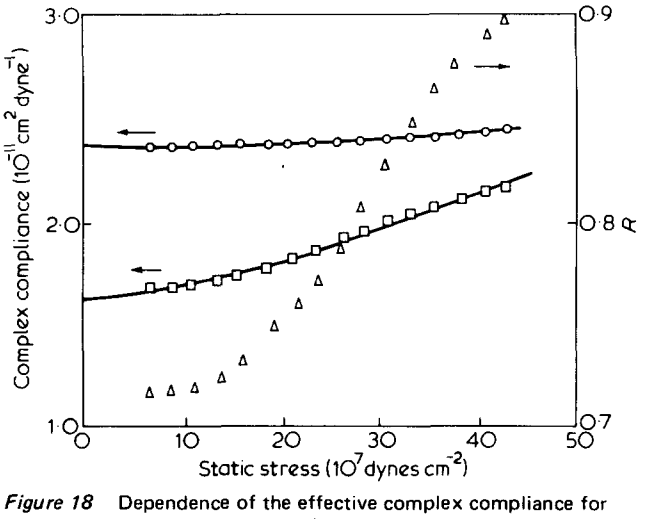

Figure 18 Dependence of the effective complex compliance for the material within the clamps (□), the complex compliance for the material between the clamps (○), and the ratio R (△), on the applied static stress for polyimide at 20°C. The frequency was 110 Hz and the stress rate ranged from 9.0×10^9 dynes cm^{-2} s^{-1} to 25.0×10^9 dynes cm^{-2} s^{-1}. The lines, drawn through the compliance data for the material between and within the clamps, were obtained using a first order and second order polynomial in static stress, respectively

Table 4 Experimental values for the ratio of the compliances within and between the clamps (R)

Material	Temperature °C	Frequency [Hz]	Stress rate [1 x 10^9 dynes cm^{-2} s^{-1}]	Static stress [1 x 10^7 dynes cm^{-2}]	*R*	Reference
Polyimide	20	11	0.8–2.3	7.0	0.6	This work
				43.0	0.82	
		110	9.0–25.5	7.0	0.71	
				43.0	0.9	
Polyethylene	20	11	0.8–2.5	2.5	0.51	
		110	9.0–33.0	2.5	0.47	
PMMA	–	11	0.9–3.7	–	$1.03/L_c$	1
		110	8.0–27.0	–	$1.22/L_c$	
Epoxy	20	11	–	–	0.83	19
PET	20	11	–	–	0.35	21
				Static strain		
SBR rubber	30	110	1.2–3.5	0.0	$0.658/L_c$	12
			1.4–5.0	0.5	$0.34/L_c$	

tween the clamps. In contrast, a second order polynomial in static stress was required to describe the behaviour observed for the complex compliance for the sample within the clamps, $|I^*_{0_{eff}}$. This result is consistent with the fact that a third term in equation (29) was required to describe the equilibrium stress–strain behaviour for the polyimide sample within the clamps. In *Figure 18*, the best fit lines obtained using the appropriate polynomials in static stress are provided. As shown, due to the increased degree of nonlinearity for the sample within the clamps, $|I^*_{0_{eff}}$ increased at a faster rate with static stress than $|S^*|$. This resulted in R increasing from 0.7 to 0.9 as the static stress was increased from 7. x 10^7 to 4.3 x 10^8 dynes cm^{-2}.

In *Table 4*, experimental values for R are given for six different materials along with the experimental conditions for each measurement. The results for polyimide and polyethylene are representative of the data discussed previously. The R values for other materials were calculated using data that have been published by other investigators[1,12,19,21], along with the values for D_{oc} determined in this work. When the length of the sample within the clamps was not given, the ratio R is provided in terms of L_c. Assuming that L_c in these studies was equal to 1 cm, the value of R was found to range between 0.3 and 1.2 for these materials. Since R less than 1, corresponds to the condition where the sample within the clamps is less compliant than the sample between the clamps, these results were considered reasonable.

The R values presented for PMMA in *Table 4* were calculated from Massa's data[1], obtained with a Rheovibron Model DDV-II. As it was observed for polyimide and polyethylene in our study, the R values obtained for Massa's PMMA data were independent of the experimental frequency. Since the compliance of a polymeric sample both within and between the clamps may be expected to show a similar dependance on frequency, the observed invariance of R with frequency is reasonable. Furthermore, since the R values for PMMA were calculated using the D_{oc} values obtained in this work, these values for D_{oc} appear to be applicable to other Model DDV-II Rheovibrons.

Figure 19 shows the temperature dependance of R for a polypropylene and an epoxy sample at 11 Hz. For both materials R was observed to decrease with increasing temperature. This result implies that the sample within

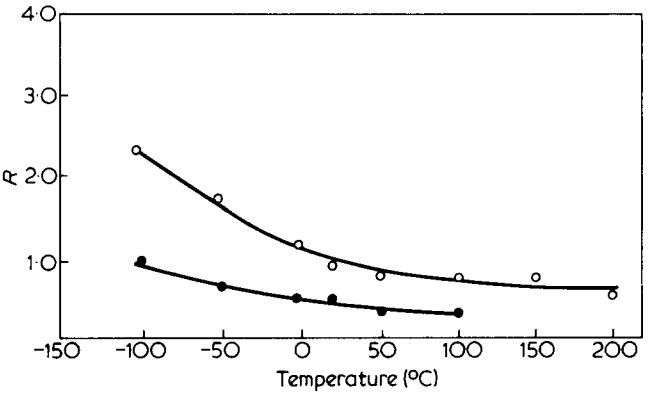

Figure 19 Dependence of the ratio (R) on temperature for a polyethylene (●) and an epoxy (○) sample. The frequency of experimentation was 11 Hz for both materials

the clamps is becoming less compliant faster than the sample between the clamps as the temperature is increased. For the other polymers that we have examined including polyethylene and polypropylene, the calculated value for the ratio was less than one for all the temperatures for which measurements were made. Although R values greater than one, imply that the material within the clamps is more compliant than the material between the clamps, a value of R as large as 2.3 was found for an epoxy sample at −100°C. This large value for R, obtained for the epoxy sample, may be due to a number of effects including (a) differences in the rate of dimensional change for the sample and the aluminium clamp with temperature, (b) shearing of the sample within the clamps, and (c) the different extents of nonlinearity observed for the sample within and between the clamps. The complicated nature of the stress–strain behaviour, for the sample within the clamps, makes it difficult to offer any one simple explanation for this large R value. Since for most of the materials examined R was found to be less than or equal to one, it is reasonable to conclude that for most materials, clamping of a sample will result in an effective complex compliance, for the sample within the clamps, which is less than the complex compliance observed for the sample between the clamps.

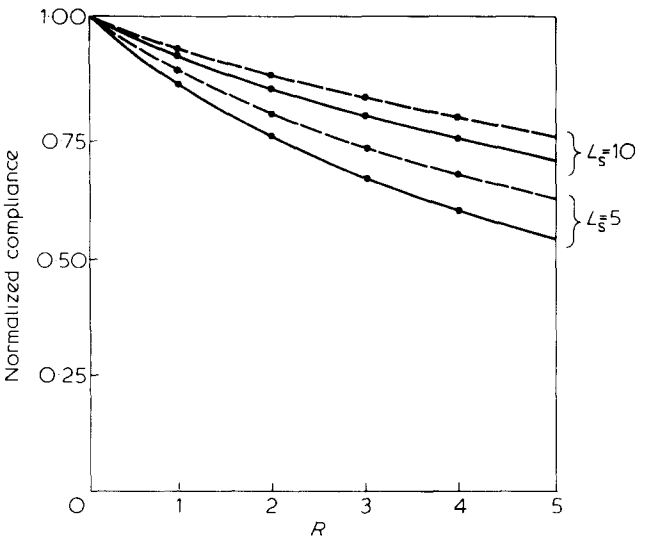

Figure 20 Normalized complex compliance of polyimide at 20°C as a function of the ratio (R) for different sample lengths within (L_c) and between the clamps (L_s). The complex compliance calculated for any value of R was normalized by dividing it by the complex compliance calculated for $R = 0$. The lines shown for each L_s value were calculated assuming (– – – –), $L_c = 0.6$ cm, and (——), $L_c = 0.8$ cm

The determination of the complex compliance and the error constant from equation (37a), requires that each sample's cross-sectional area be kept constant as different geometry samples are tested. However, by combining equations (37a), (40), and (41) the following general expression can be derived:

$$D(AF)(1+W) = B|S^*|\left(\frac{L+RL_c}{A}\right) + D_{oc} \qquad (42)$$

This equation can be used to analyse data obtained with samples having different cross-sectional areas if D_{oc} and L_c are known. Furthermore, with the aid of equation (42) a sample's measured complex compliance, $|S^*|$, can be normalized with its value that would result if the ratio R was set to zero (i.e. $|S^*|_{R=0}$). This normalization procedure of a sample's complex compliance defines a normalized complex compliance of a sample:

$$\frac{|S^*|}{|S^*|_{R=0}} = \frac{L}{L+RL_c} \qquad (43)$$

that depends on the specific polymer tested only through the ratio R since L and L_c refer to the sample's length between and within the clamps. To provide a feel for the normalized complex compliance, equation (43) was plotted in *Figure 20* as a function of R at two different lengths for the sample within and between the clamps. As expected, *Figure 20* shows that the normalized complex compliance decreases with increasing R. Furthermore this figure shows that the dependance of the measured complex compliance on R decreases as either the sample length is increased or the length of sample within the clamps is decreased. Since R was found to be less than one for most of the polymers examined, equation (42) can be used to obtain an excellent approximation of the sample's complex compliance from a single measurement. For example, if the sample length within and between the clamps are $L_c = 0.8$ and $L = 10.0$ cm, respectively and R is assumed to be $R = 0.5$, for a polymer whose R value actually ranges between 0 and 1, the maximum error due to assuming this R value would be $\pm 4\%$. Even if the polymer's actual R value was as large as 2.3, as found for epoxy at -100 C, the error due to this incorrect estimation of R would still be only $\pm 13\%$. Thus, an excellent approximation of the sample's complex compliance, for any polymer, may be obtained from a single measurement. However, it should be recalled that this value of the sample's complex compliance may still depend on the static stress and stress rate imposed during the measurement.

THE MEASURED LOSS TANGENT AND THE COMPONENTS OF THE COMPLEX COMPLIANCE

The analysis so far has concentrated in providing a general description for the determination of a sample's complex compliance on an instrument free basis. However, for the complete description of a polymeric sample's dynamic mechanical properties, the sample's loss tangent on an instrument free basis (i.e. tan δ) must also be determined. Once a sample's complex compliance and tan δ, have been determined, its dynamic mechanical properties, expressed in storage and loss compliance, can be calculated with equation (13). The influence then of the applied static stress and stress rate on the storage and loss compliance can be accounted for quantitatively through the model equations (equation (20) and (21)) that have been provided. In what follows, this procedure is carried out in detail for the polyimide sample at 20°C whose complex compliance was provided as a function of static stress and range of stress rates at 11 and 110 Hz frequencies.

To calculate the storage and loss compliances of polyimide samples, their instrument free loss tangent, tan δ must be determined at each level of static stress and stress rate that were used for measurements. Since the Rheovibron provides the measured loss tangent (tan α) directly, the experimental conditions applied during each measurement can be explicitly specified. In particular, unlike the complex compliance which was provided for a range of stress rates, the exact stress rate under which each tan α was measured can be defined. In *Figure 21*, tan α for polyimide at 20°C is provided at five different stress rates as a function of the applied static stress for data taken at 11 and 110 Hz. Tan α was observed to increase with both increased static stress and stress rate, ranging in the interval $0.01 \leqslant \tan\alpha \leqslant 0.024$ over the range of experimental conditions studied.

The tan α values shown in *Figure 21* were corrected to their instrument free equivalents (i.e. tan δ's) by the application of Massa's correction (equation (9b)). Using these values for tan δ, the appropriate values for the complex compliance given in *Table 3*, along with equations (13) and (14), the storage and loss components of the complex compliance were calculated on the instrument free basis. The results of these calculations are presented in *Figures 22* and *23*, where S' and S'' are plotted as a function of the applied static stress and stress rate. In these figures, it should be noted that since, for tan $\delta < 0.1$ the storage component is approximately equal to the magnitude of the complex compliance ($S' = |S^*|$), S' is provided for the same range of stress rates used for the determination of $|S^*|$. In contrast, for the same sample, S'' is

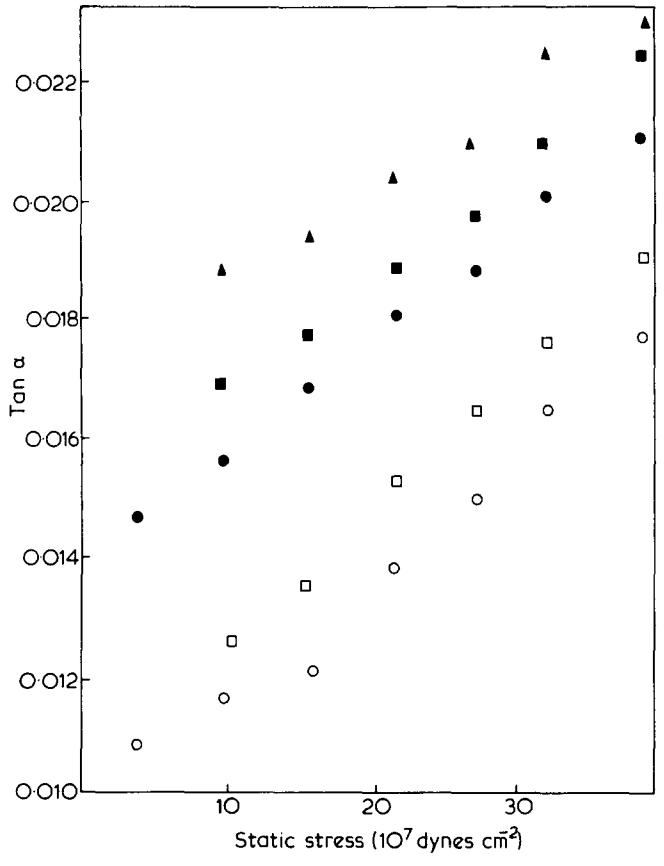

Figure 21 Measured loss tangent, tan α, for polyimide at 20°C as a function of the applied static stress. The stress rates used were: ○, 1.06; □, 3.0; ●, 10.4; ■, 32.5; and ▲, 45.8; in units of 10^8 dynes cm^{-2} s^{-1}. Frequencies used were 11 and 110 Hz and are denoted by the open and solid symbols respectively

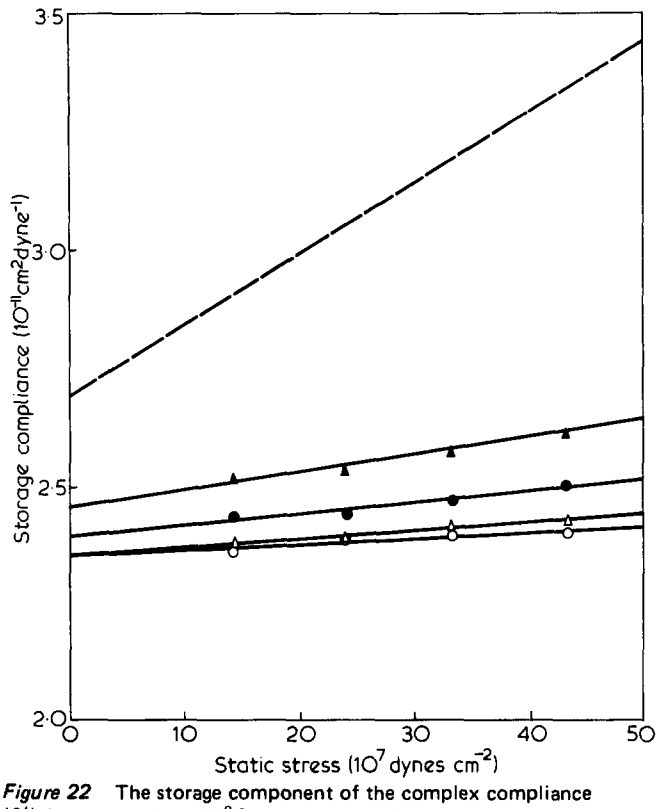

Figure 22 The storage component of the complex compliance (S') for polyimide at 20°C as a function of the applied static stress. Frequencies used were 11 and 110 Hz and are denoted by the solid and open symbols respectively. The range of stress rates at which each data point was obtained were: ▲, 0.85–1.77; ●, 2.7–4.6; △, 9.2–25.5; and ○, 29.7–63.6; in units of 10^8 dynes cm^{-2} s^{-1}. The lines drawn were determined by least squares regression of equation 20. The equilibrium compliance (— —) is also plotted for comparison

directly proportional to the loss tangent which exhibited a strong dependence on the applied stress rate. Thus the experimental conditions (i.e., static stress, frequency, and stress rate) at which each tan α was measured could be directly correlated with the calculated S'' values (see *Figure 23*). For each stress rate or range of stress rates the data in *Figures 22* and *23* were fitted by least squares regression of equation (20). The excellent fits shown in *Figures 22* and *23* further support the contention of Mason that a model which is capable of describing the equilibrium nonlinear stress–strain behaviour can be extended to the dynamic problem. In *Table 5* the material descriptors U'_1, U'_2, U''_1 and U''_2 of equation (20) for polyimide are provided as a function of frequency and stress rate. As shown in *Figure 22*, the storage part of the complex compliance was found to increase with decreasing stress rate approaching the values determined for the static analysis. The degree of sample nonlinearity, as indicated by the slope of the lines given in *Figure 22*, increased with decreasing stress rate. These results are consistent with the behaviour generally observed for a polymer's stress–strain response as a function of the experimental rate. The loss component of the complex compliance, was found to increase with both applied static stress and stress rate. As shown in *Figure 23*, the value for S'' at 110 Hz varied by as much as 80% over the range of static stress levels and stress rates investigated.

If the zero static stress material descriptors U'_1 and U''_1 determined at each stress rate are extrapolated to zero stress rate a measure of the material descriptors which are independent of the applied experimental conditions will

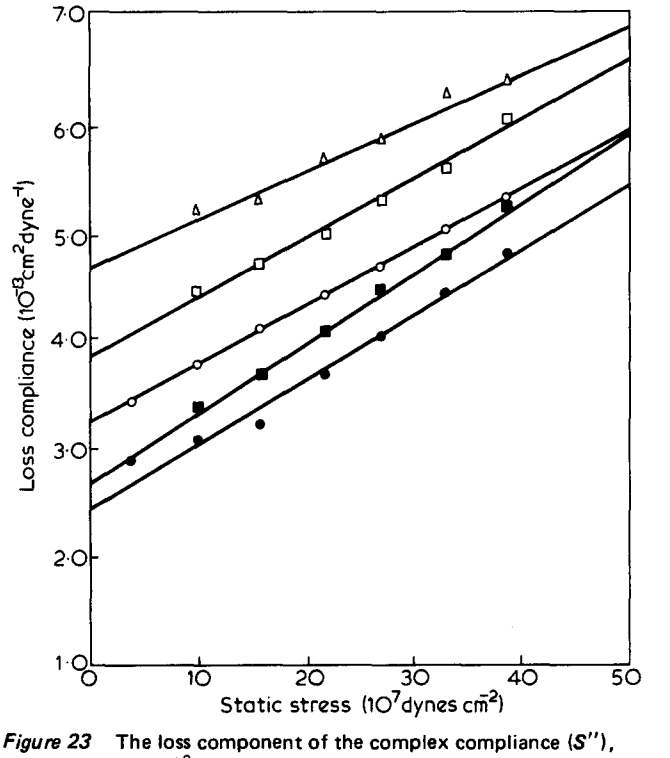

Figure 23 The loss component of the complex compliance (S''), for polyimide at 20°C, as a function of the applied static stress. Frequencies used were 11 and 110 Hz and are indicated by the solid and open symbols respectively. The stress rates at which the data points were obtained are: ●, 1.06; ■, 3.0; ○, 10.4; □, 32.5; and △, 45.8; in units of 10^8 dynes cm^{-2} s^{-1}. The lines drawn through the data were determined by least squares regression of equation 20

Table 5 Dependence of the material descriptors for polyimide at 20°C, on frequency and stress rate

Frequency [Hz]	Stress rate [1 x 10^9 dynes cm^{-2} s^{-1}]	$U'_1 \times 10^{11}$ [cm^2 $dyne^{-1}$]	$U'_2 \times 10^{21}$ [cm^2 $dyne^{-1}]^2$	$U''_1 \times 10^{13}$ [cm^2 $dyne^{-1}$]	$U''_2 \times 10^{22}$ [cm^2 $dyne^{-1}]^2$
11	0.83	2.46	0.9	2.53	2.74
11	1.06	2.46	0.9	2.49	2.95
11	3.0	2.39	0.63	2.71	3.23
110	10.4	2.35	0.45	3.28	2.62
110	13.0	2.35	0.45	3.32	2.54
110	20.0	2.35	0.45	3.73	2.27
110	32.5	2.35	0.34	3.88	2.68
110	41.3	2.35	0.34	4.68	2.17
110	45.8	2.35	0.34	4.71	2.20

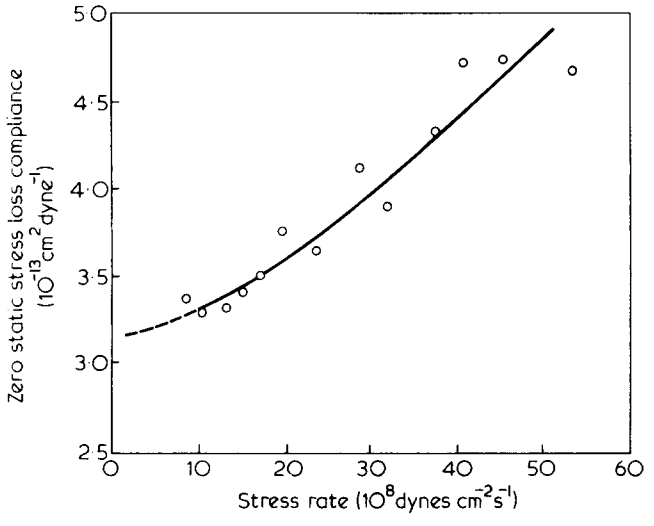

Figure 24 The zero static stress material descriptor U''_1, for polyimide at 20°C and 110 Hz, as a function of stress rate. The broken line (— — — —) shows an extrapolation to zero stress rate

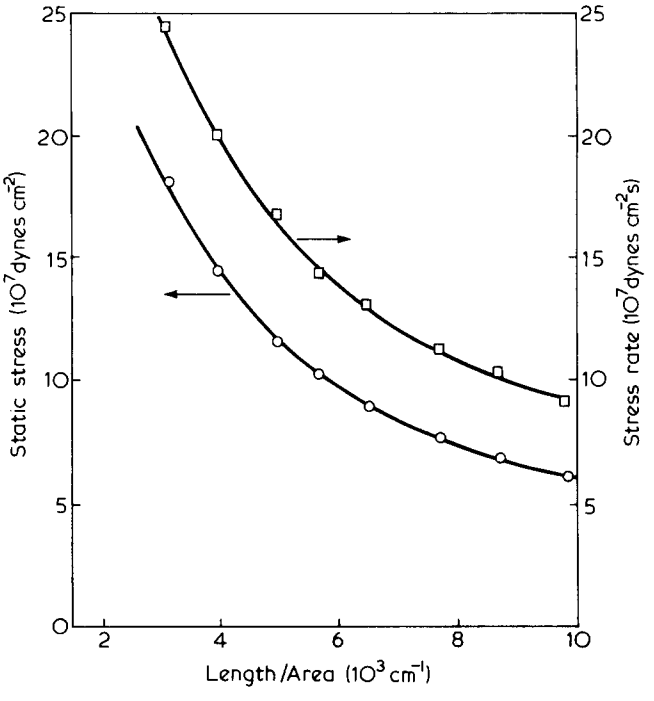

Figure 25 Static stress and stress rate imposed on a polyimide sample as a function of sample geometry (*L/A*). The sample's cross-sectional area was (*A* = 1.046 x 10^{-3} cm^2) and the oscillating displacement was 0.005 cm

be provided for a range of stress rates. These values for each range can be extrapolated to zero stress rate with reasonable accuracy since the dependence of U'_1 on stress rate was small. This extrapolation gave $U'_1 = 2.49 \times 10^{-11}$ at 11 Hz and $U'_1 = 2.35 \times 10^{-11}$ at 110 Hz as the zero static stress values of U'_1 at zero stress rate. (See *Figure 22* and *Table 3*). The zero static stress values for U''_1 were also extrapolated to the zero stress rate as illustrated in *Figure 24* for the 110 Hz data. As indicated by the broken line in *Figure 24* this extrapolation provided a value of 3.18 $\times 10^{-13}$ for U''_1. From the values of U''_1 and U'_1, tan δ at zero stress rate was calculated to be $U''_1/U'_1 = 0.0135$. Applying the procedure discussed above, to the 11 Hz data U''_1 and tan δ were calculated to be 2.39×10^{-13} and 0.0096 respectively.

The reader is cautioned of the possible errors which can result from the extrapolation of the dynamic data described above. Since we have offered no model to describe the dependance of the zero static stress parameters on stress rate the extrapolated values may be fortuitous. Also the above extrapolation procedure doesn't allow for the possibility that there may exist a set of critical combinations of static stress and stress rate at which the properties would be independent of these experimental conditions. The implication of course is that at small enough static stress levels and low enough stress rates, the sample's viscoelastic response will become linear. If this were the case, the values for the zero stress U'_1, U''_1 and tan δ obtained above would be slightly underestimated.

Finally, to explain the observed dependance of the measured dynamic mechanical properties on the sample's geometry the following experiment was performed. The dynamic mechanical properties were measured as a function of L/A for polyimide at 20°C and 110 Hz. The amplitude of oscillation was kept constant at 0.005 cm, while the static stress was determined by balance procedure one. Application of the balance procedure one resulted in a static displacement which ranged from 0.015–0.02 cm, irrespective of the sample length used. The sample's cross-sectional area was 1.06×10^{-4} cm and the geometric parameter was varied by changing the sample length from 10.3 to 3.3 cm. These different sample lengths resulted in changing the applied static stress and stress rate to be applied on the polymer as shown in *Figure 25*. Using equations (9b) and (20), these values for the experimental conditions, the material descriptors given in *Table 5* along with values at other stress rates not presented and the measured dynamic force, tan α was calculated as a function of L/A. These values were used to generate the continuous line shown in *Figure 26*. As can be seen from *Figure 26* the measured values for tan α are in

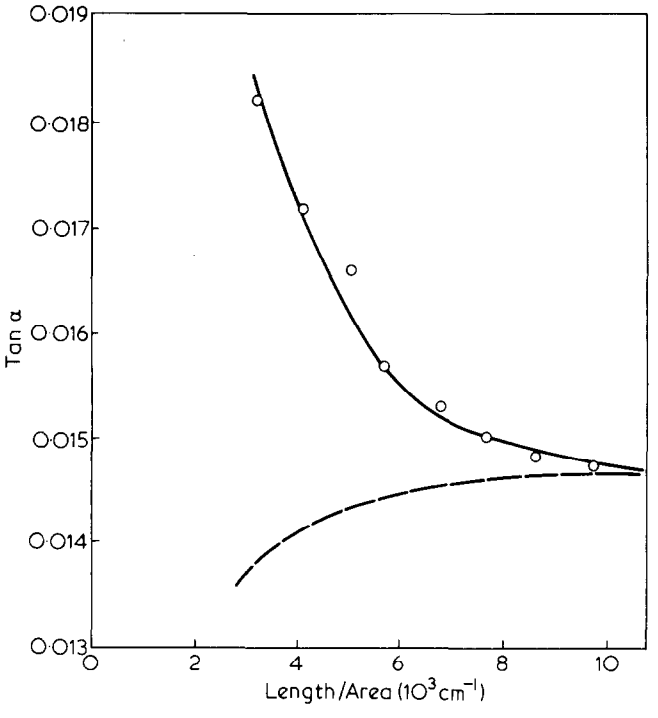

Figure 26 Dependence of the measured loss tangent (tan α) on sample geometry (L/A) for polyimide at 20°C and 110 Hz. Experimental data are shown by (○). The model prediction using the material descriptors (U_1', U_2'', U_1', U_2'') and the static stress and stress rate profiles of *Figure 25* are shown by (——). Massa's[1] prediction accounting for the instrument components only, is shown by (– – – –)

good agreement with the values calculated from the model parameters and the experimental conditions given in *Figure 25*.

The measured loss tangent was observed to decrease with increasing L/A, approaching asymptotically the tan δ value of 0.0135 obtained by the extrapolation discussed earlier. For comparison, the prediction of Massa's mechanical model is given. This prediction was obtained following the procedure outlined by Massa[1], assuming an instrument free value for tan $\delta = 0.0151$. These results explicitly demonstrate the importance of accounting for the experimental conditions and the sample material's response during measurements with the Rheovibron.

CONCLUSION

This study was aimed at providing a comprehensive description of the Rheovibron viscoelastometer's operation so that reproducible and instrument independent dynamic mechanical properties of polymers can be obtained. Prior to this study, efforts that described the effects of either the instrument's components or the experimental conditions on the measured dynamic mechanical properties had been made. The present study has shown that these effects are coupled to the polymeric sample size being tested and must be accounted for if the measured dynamic mechanical properties are to reflect those of the polymer from which the sample was taken.

To provide a quantitative description of the experimental conditions under which dynamic mechanical measurements are made with the Rheovibron, it was found necessary to make several minor but essential modifications to the instrument. The clamp and chamber modifications coupled with the electronic modifications, which allowed for the monitoring of several experimental parameters, assured data reproducibility within 5%. Specifically, the electronic modifications made possible the determination of the applied static stress imposed on the sample during a measurement.

The importance of monitoring the static stress level during an experiment with the Rheovibron, lead to an unambiguous balancing procedure that could be explained in terms of the polymers nonlinear stress strain response.

The recognition that the Rheovibron can impose conditions under which a polymeric sample may exhibit nonlinear stress–strain behaviour also formed the basis by which the dynamic mechanical data were analysed. The analysis was performed by modelling the materials nonlinear response in terms of a simple series expansion of the properties in stress. Application of this model to polymeric materials, under the equilibrium and dynamic conditions that are imposed with the Rheovibron during measurement, demonstrated that their dynamic mechanical properties will be uniquely determined only when the temperature, frequency, static stress, and stress rate are specified. This procedure for the determination of the dynamic mechanical data was explicitly demonstrated using polyimide as an example. In particular, the measured complex compliance for polyimide at 20°C and at frequencies of 11 and 110 Hz were shown to have a dependence on the applied static stress and stress rate. The measured complex compliance at each level of stress and stress rate was corrected for the instrument's compliance and for an effective compliance that had been associated with the sample in the clamps. The identification and use of an effective compliance for the sample in the clamps provided a general procedure for the determination of the error constant for the material D_{ov} and the instrument D_{oc}. As a result of this procedure, which was also employed for a variety of other polymers in addition to polyimide, it is now possible to estimate the error constant required in the Rheovibron calculations from a single measurement if the proper sample dimensions and experimental conditions are used.

Armed with a value of the constant component of the error constant as well as the values for tan α and the sample's complex compliance, the storage and loss compliance of the sample can be calculated on an instrument free basis using the procedure of Massa. However, these values will continue to have a dependence on the experimental conditions imposed during the measurement, such as the temperature, frequency, static stress, and stress rate. To reflect the materials true dynamic mechanical properties, the sample's properties are extrapolated with the proposed model to a stress free state, so that their dependence is only on the temperature and frequency of experimentation.

In conclusion, the present study of the Rheovibron has shown that commercial instruments that are used for measuring dynamic mechanical properties of polymers must be thoroughly investigated before any implication about material properties are made. One has to caution that with more and more automated instruments coming on the market, the investigator should always examine how the assumptions inherent in the instrument's design and operation can affect a particular polymer. Only when such an investigation has been made as the one performed here with the Rheovibron, one can have confidence that

the true dynamic mechanical properties of the material have been measured.

ACKNOWLEDGEMENTS

The following individuals and organizations are acknowledged for their contribution during the course of this work: H. J. Wyatt for his assistance in upkeeping and modifying the Rheovibron electronics, E. J. Tolle of IMASS for helpful discussions, assistance, and continued interest in this work, J. T. Hoggatt and the Boeing Aerospace Company for donating their Rheovibron to our research programme. Financial support during the major part of this study was provided by the National Science Foundation-Polymers Program Grant No. DMR-7822108, while initial funds were provided by the Graduate School Research Foundation of the University of Washington.

REFERENCES

1 Massa, D. J. *J. Appl. Phys.* 1973, **44**, 2595
2 Massa, D. J. *A.C.S. Coat and Plast. Prep.* 1975, **35**, 371
3 Murayama, T. *J. Appl. Poly. Sci.* 1975, **19**, 3221
4 Locati, G. *Polym. Eng. Sci.* 1978, **18**, 793
5 Murayama, T. and Silverman, B. *J. Appl. Polym. Sci.* 1975, **19**, 1695
6 MacLean, D. L. and Murayama, T. *Trans. Soc. Rheol.* 1974, **18**, 237
7 Yee, A. F. and Takemore, M. T. *J. Appl. Polym. Sci.* 1977, **21**, 2597
8 Kenyon, A. S. *et al.*, *A.C.S. Polym. Prepr.* 1976, **17**, 7
9 Samuels, R. J. 'Structured Polymer Properties', Wiley, New York, 1974
10 Seferis, J. C., McCullough, R. L. and Samuels, R. J. *Appl. Polym. Symp.* 1975, **27**, 205
11 Seferis, J. C., McCullough, R. L. and Samuels, R. J. *Polym. Eng. Sci.* 1976, **16**, 334
12 Seferis, J. C., McCullough, R. L. and Samuels, R. J. *J. Macromol. Sci. Phys.* 1977, **B13(3)**, 357
13 Takayanagi, M. *Mem. Fac. Eng.* 1963, **23**, 1
14 Rheovibron DDV-II Instrument Manual (IMASS)
15 Voet, A. and Morawski, J. C. *Rubber Chem. Tech.* 1974, **47**, 758
16 Litt, M. H. and Torp, S. *J. Appl. Phys.* 1973, **44**, 4282
17 Wedgewood, A. R. and Seferis, J. C., in preparation
18 Coulis, P. A. *MS Thesis*, University of Washington, 1979
19 Keenan, J. D. *MS Thesis*, University of Washington, 1979
20 Keenan, J. D., Seferis, J. C. and Quinlivan, J. T. *J. Appl. Polym. Sci.* 1979, **24**, 2375
21 Bomberger, T. *Senior Thesis*, University of Delaware 1977
22 Ramos, A. R., Bates, F. S. and Cohen, R. E. *J. Polym. Sci. Polym. Phys. Edn.* 1978, **16**, 753
23 Love, A. E. H. 'Mathematical Theory of Elasticity', Dover Reprints, New York, 1944
24 Arridge, R. G. C. and Folkes, M. J. *Polymer* 1976, **17**, 495
25 Horgan, C. O. *Int. J. Solids Struc.* 1974, **10**, 837
26 Lewis, E. L. V. *J. Mater. Sci.* 1979, **14**, 2343
27 Mason, P. *J. Appl. Polym. Sci.* 1959, **1**, 63
28 Mason, P. *J. Appl. Polym. Sci.* 1961, **5**, 428
29 Sadd, M. H. and Morris, D. H. *J. Appl. Polym. Sci.* 1976, **20**, 421
30 Kobayashi, A. and Ohtani, N. *J. Appl. Polym. Sci.* 1971, **15**, 975
31 Ferry, J. D. 'Viscoelastic Properties of Polymers', Wiley, New York, 1970
32 Hearmon, R. F. S. 'An Introduction to Applied Anisotropic Elasticity', Oxford University Press, 1961
33 Perry, J. H., Chilton, C. H. and Kirkpatrick, S. D. 'Chemical Engineer's Handbook', McGraw Hill, 1972
34 'Modern Plastic Encyclopedia', McGraw Hill, 1972
35 Treloar, L. R. G. 'The Physics of Rubber Elasticity', Clarendon Press, London, 1958
36 Rheovibron DDV-II Maintenance Manual, (IMASS)
37 Kreyszig, E. 'Advanced Engineering Mathematics', Wiley, New York, 1968
38 Ritger, P. D. and Rose, N. J. 'Differential Equations with Applications', McGraw Hill, New York, 1968

APPENDIX

Auxiliary experimental techniques

An oscilloscope can be easily attached to the Rheovibron, allowing the operator to visually monitor the instrument's operating status. This is particularly useful when operating above or below ambient temperature, where visual observation of the sample, which is enclosed in the sample chamber, is not possible. An understanding of the various Lissajous figures, observed on the oscilloscope, enables the operator to detect a variety of conditions including sample shrinkage, misalignment, and vibration modes. Since all of these conditions influence the properties measured, their detection and elimination are essential for accurate and reproducible instrument operation. In the sections that follow, a detailed explanation of the Lissajous figures observed for each operating position of the main selector switch and an example of their application for the detection of vibration modes is provided.

Lissajous figures. The Lissajous figures observed while operating the Rheovibron result from plotting two time dependent voltages against each other. One of these voltages is an internally generated reference signal and can be described by the following equation:

$$V_x = A \sin \omega t \qquad \text{(A1)}$$

where A is the amplitude and ω is the angular frequency.

The second voltage signal depends on the operation mode of the instrument. In the following, the voltage signals expected during operation in the amplitude factor (AF), dynamic force (DF), and tan δ positions of the main selector switch are discussed. From this information the Lissajous figures expected, during operation in each main selector switch position, can be generated for comparison to the experimentally observed figures.

When operating in the amplitude factor position (AF) of the main selector switch, the signal from the T7 gauge is plotted against the reference signal. Although this signal has the same amplitude as the reference signal, they are generally out of phase from each other. Representing the phase angle lag by α, the signal from the T7 gauge can be written as:

$$V_y = A \sin(\omega t + \alpha) \qquad \text{(A2)}$$

A plot of the T7 gauge signal against the reference signal results in an open loop figure on the oscilloscope. The size of this loop is a function of α, with a diagonal line being observed for $\alpha = 0$ and a circle for $\alpha = \pi/2$.

When operating in the dynamic force position, of the main selector switch, the voltage response from the T1 stress gauge is plotted against the reference signal. When the instrument is properly balanced the T1 gauge signal has the same amplitude and is in phase with the reference signal, viz.,

$$V_y = A \sin \omega t \qquad \text{(A3)}$$

A plot of the reference signal (see equation (A1)) on the x axis and the signal from the T1 gauge on the y axis, results in a diagonal line on the oscilloscope as discussed in the instruction manual[14]. The use of this Lissajous figure as an aid for instrument balance and phase adjustment is also discussed in the instruction manual.

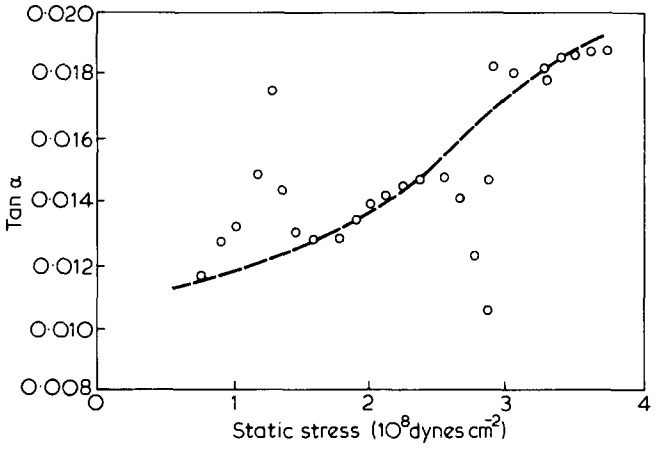

Figure 27 Dependence of the measured loss tangent (tan α) on static stress for polyimide at 20°C and 11 Hz. Normal behaviour (vibration free) is shown by the broken line. Positive and negative deviations from the normal behaviour are attributed to resonant vibrations

During operation in the tan δ position, of the main selector switch, the difference between the T1 and T7 gauges output voltage signals is plotted against the reference signal. This signal difference can be written as:

$$V_y = A\,[\sin \omega t - \sin(\omega t + \alpha)] \qquad \text{(A4)}$$

The resulting Lissajous figures depend on α and can be easily generated for comparison with the experimentally observed figures.

In addition to providing a means for visually monitoring the instrument's status during operation in the amplitude adjust, dynamic force, and tan δ positions, of the main selector switch, the Lissajous figures can also be used during the C–R balance steps[14] for the T1 and T7 gauges. When the C–R balance has been properly completed a horizontal line is observed on the oscilloscope.

During measurement of the dynamic mechanical properties with the Rheovibron vibrational modes, sample misalignment, etc., can cause the Lissajous figures to be distorted from their expected forms. An understanding of these signals enables the Rheovibron operator to detect and eliminate these operating problems. Therefore, it is recommended that the electrical modification, of the main selector switch, discussed in the text be made, and that the monitoring of these Lissajous figures be a standard operating procedure. It is unfortunate that no precise method has been published, which would allow an operator to assign the various distortions of the Lissajous figure to a unique cause. This area would be fruitful for further study. In particular, a description of the Lissajous figures, which result due to the vibrations caused by the instrument's resonance, would be very useful.

Vibration modes

To illustrate the importance of using the Lissajous figures to detect experimental problems, the effect of vibrations on the measured loss tangent (tan α), for a polyimide sample at 20°C and 11 Hz, is provided here as an example. As shown in *Figure 27*, tan α was observed to gradually increase with increased static stress until the onset of vibrations at a static stress value of 1×10^8 dynes cm^{-2}. These vibrations were observed both visually and by distortion of the Lissajous figures. At this static stress level the loss tangent (tan α) increased rapidly with increasing static stress. Damping the vibration, by slightly touching the sample rod, resulted in the removal of this vibration. Vibration free values of tan α are indicated in *Figure 27*, by the dashed line. Without touching the rods, this vibration was removed by increasing the applied static stress. The measured loss tangent decreased, with the removal of this vibration, to a value which was considered consistent with the expected material behaviour. Upon continued increase of the applied static stress the system entered a second regime of vibrations, which this time resulted in a decrease in the measured loss tangent. Again damping the system, by slightly touching the rods, resulted in the removal of this vibration. As expected, the measured tan α again approached its vibration free value. Further increases in the static stress, without touching the rods, eliminated the fluctuations of tan α. It should be noted that operation with the same sample at 3.5, and 110 Hz was found to be free of vibrations.

The vibrations may be attributed to a system instability or a resonance mode. For the Rheovibron, which is a forced oscillation instrument, the longitudinal and lateral resonance modes may be assumed to be coupled. Thus a complete analysis of the instrument's resonance is quite complex and is beyond the scope of this work. However, separate considerations of the longitudinal and lateral vibration modes lead to the following qualitative explanation for the tan α anomalies presented in *Figure 27*.

For the longitudinal vibrations a simple mechanical model, that consists of a spring with a mass in series with a dashpot was considered. For this mechanical system, the resonance frequency ω_r, can be obtained in terms of model parameters as:

$$\omega_r = \left(\frac{K}{M} - \frac{C^2}{2M^2}\right)^{1/2} \qquad \text{(A5)}$$

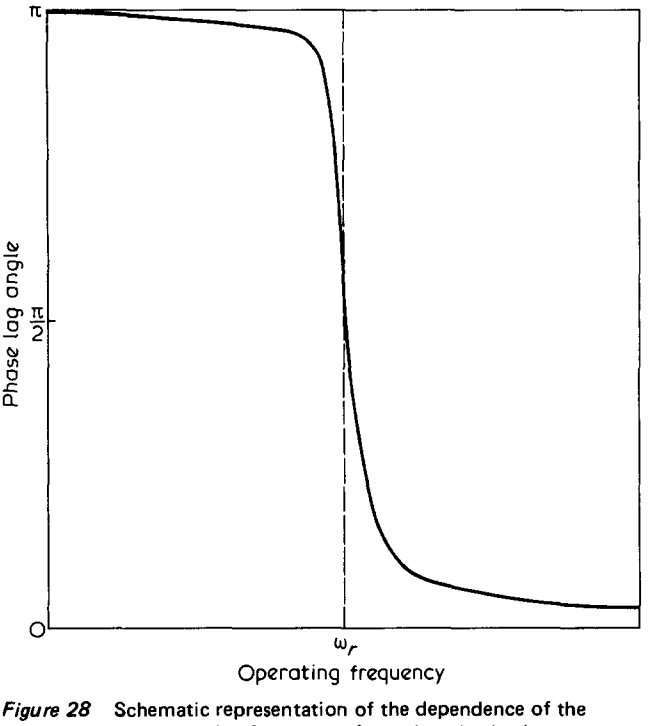

Figure 28 Schematic representation of the dependence of the phase lag on the operating frequency, for a viscoelastic element consisting of a spring with mass connected in series to a dashpot. The resonance frequency of this element is identified by ω_r. The solid line shows the response expected for a damped system while the broken line shows the response expected for an undamped system

where K is the spring constant, M is the mass, and C is the dashpot constant[37,38]. For lateral vibrations, a vibrating string under tension was considered. The resonance frequency ω_r, for this system is given as[38]:

$$\omega_r = \frac{r\pi T}{\sqrt{\rho l}}; \quad r = 1, 2, 3, \ldots \tag{A6}$$

where T is the applied tension, l is the length and ρ is the density of the string. Recalling that for a nonlinear material K is a function of the applied tension, it can easily be seen from equations (A5) and (A6) that both the longitudinal and lateral resonance frequencies are changed as the tension applied to the sample is varied.

To illustrate the possible effects of changing the resonance frequency of the instrument, the spring with mass in series with a dashpot is considered in more detail. If the resonance frequency for this system is changed such that its value crossed the value of the operating frequency a phase shift occurs. For an ideally undamped system (i.e. $C = 0$), this phase shift is equal to π and would result in no variation of the measured loss tangent. However, if the system is damped this phase shift will occur over a range of frequencies as shown in *Figure 28*. This would result in either decreasing or increasing the measured loss tangent depending on which side of the operating frequency the resonance frequency is located.

From the above simplified analysis it can be inferred that the type of polymer being measured, the material's dimensions, and/or the tension applied on the sample may result in altering the systems resonance frequency. Operation at or near the systems resonance frequency can result in system vibrations which can cause errors in the measured properties. Also as it was shown earlier, a system resonance may occur at operating frequencies other than 35 Hz, which has been considered the Rheovibron's resonance frequency. Furthermore, the use of different sample dimensions can result in the elimination of vibrations by shifting the system's resonance. In addition, the Rheovibron like the vibrating string can have multiple resonances (i.e. harmonics), making *a priori* predictions of the operating frequencies, without a detailed model, an impossible task. However, awareness of these vibration modes has allowed for their detection and in some cases their elimination, leading to improved instrument stability and improved data reproducibility.